



**3-DIMENSIONAL MOVING LOAD
PROBLEMS FOR ELASTIC AND
COATED ELASTIC HALF-SPACES**

PhD Dissertation

Onur ŞAHİN

Eskişehir, 2016

**3-DIMENSIONAL MOVING LOAD PROBLEMS FOR ELASTIC
AND COATED ELASTIC HALF-SPACES**

ONUR ŞAHİN

PhD DISSERTATION

Department of Mathematics

Supervisor: Assoc. Prof. Dr. Barış ERBAŞ

Eskişehir

Anadolu University

Graduate School of Science

May, 2016

JÜRİ VE ENSTİTÜ ONAYI
(APPROVAL OF JURY AND INSTITUTE)

Onur ŞAHİN'in "**3-Dimensional Moving Load Problems for Elastic and Coated Elastic Half-Spaces**" başlıklı tezi 18/05/2016 tarihinde, aşağıdaki jüri tarafından değerlendirilerek "Anadolu Üniversitesi Lisansüstü Eğitim-Öğretim ve Sınav Yönetmeliği"nin ilgili maddeleri uyarınca, **Matematik** Anabilim dalında Doktora tezi olarak kabul edilmiştir.

	<u>Ünvanı-Adı Soyadı</u>	<u>İmza</u>
Üye (Tez Danışmanı)	: Doç. Dr. Barış ERBAŞ
Üye	: Prof. Dr. Cem YÜCE
Üye	: Prof. Dr. Elçin YUSUFOĞLU
Üye	: Doç. Dr. Nihal EGE
Üye	: Doç. Dr. Dursun IRK
	
		Enstitü Müdürü

ABSTRACT

3-DIMENSIONAL MOVING LOAD PROBLEMS FOR ELASTIC AND COATED ELASTIC HALF SPACES

Onur ŞAHİN

Department of Mathematics

Anadolu University, Graduate School of Science, May, 2016

Supervisor: Dr. Barış ERBAŞ

This study deals with 3-dimensional analysis of a point load moving at a constant speed along the surface of elastic and coated elastic half-spaces. Formulation of the problems is based on the framework of an asymptotic hyperbolic-elliptic model for the wave field developed to extract the contribution of surface waves. The validity of the model is restricted to the range of speeds close to the surface Rayleigh wave speed for both problems. It is also assumed that for the coated half-space the thickness of the coating is small compared to a typical wavelength of the surface wave.

First, the uncoated elastic half-space problem is considered and both sub and super-Rayleigh cases are studied. The surface solutions for both cases are obtained through the fundamental solution of the differential operators. Then these solutions are restored over the interior of the half-space by the means of Poisson's formula. Thus the steady-state near-field solutions are derived in terms of the elementary functions. Finally numerical computations based on the derived approximate formulae are presented.

In the coated half-space problem the surface solutions are given in integral forms obtained through the use of integral transforms for sub and super-Rayleigh cases. Then the integral solutions of the perturbed wave equation describing wave propagation along the surface are derived with their far-field asymptotic expansion using the uniform stationary phase method. Finally, numerical comparisons of exact and asymptotic results are presented for both cases.

Keywords: 3-dimensional elasticity, Moving load, Rayleigh wave,
Asymptotic model, Thin coating.

ÖZET

KAPLAMALI ve KAPLAMASIZ ELASTİK YARI UZAYLAR İÇİN 3-BOYUTLU HAREKETLİ YÜK PROBLEMİ

Onur ŞAHİN

Matematik Anabilim Dalı

Anadolu Üniversitesi, Fen Bilimleri Enstitüsü, Mayıs, 2016

Danışman: Dr. Barış ERBAŞ

Bu çalışmada kaplamalı ve kaplamasız elastik yarı uzayların yüzeylerinde sabit bir hızla hareket eden noktasal yükleri 3-boyutlu analizi ele alınmıştır. Problemin formülasyonu yüzey dalgalarının katkısını ortaya çıkarmak için geliştirilen bir hiperbolik-eliptik asimptotik modele dayanmaktadır. Her iki problem için de modelin geçerliliği Rayleigh dalga hızına yakın hız aralıklarında geçerlidir. Ayrıca kaplamalı yarı uzay için kaplamanın kalınlığının tipik yüzey dalga boyuna kıyasla küçük olduğu varsayılmıştır.

İlk olarak kaplamasız elastik yarı uzay problemi ele alınmış ve sub ve süper-Rayleigh durumları çalışılmıştır. Her iki durum için yüzey çözümleri diferansiyel operatörlerin temel çözümleri yardımıyla elde edilmiştir. Daha sonra bu çözümler Poisson formülü yardımıyla yarı uzayın iç bölgesine genişletilmiştir. Böylece kararlı-hal yakın-alan çözümleri temel fonksiyonlar cinsinden türetilmiştir. Son olarak türetilen yaklaşık formüllere dayanan sayısal hesaplamalar verilmiştir.

Kaplamalı yarı uzay probleminde sub ve süper-Rayleigh durumları için yüzey çözümleri integral dönüşümleri kullanılarak integral formda elde edilmiştir. Daha sonra yüzey boyunca yayılmayı tanımlayan pertürbe edilmiş dalga denkleminin integral çözümleri düzgün durağan faz metodu kullanılarak uzak alan asimptotik açılımları ile türetilmiştir. Son olarak her iki durum için tam ve asimptotik sonuçlar için sayısal karşılaştırmalar verilmiştir.

Anahtar Sözcükler: 3-boyutlu elastisite, Hareketli yük, Rayleigh dalgası, Asimptotik model, İnce kaplama.

ACKNOWLEDGMENTS

I would like to express my sincere gratitude to my supervisor Barış Erbaş for his guidance, encouragement and support throughout my PhD study and research. I would also like to thank him especially for giving me the opportunity to work with him on this subject. In addition to my supervisor, I am grateful to Assoc. Prof. Dr. Nihal Ege for the support and guidance she provided.

I would like to express my pleasure to Prof. JD Kaplunov and Dr. DA Prikazchikov for their invaluable comments and constructive suggestions during my research.

I am very grateful for the financial support of The Scientific and Technological Research Council of Turkey (TUBİTAK) PhD Scholarship Programme-2211 during my study.

Finally, I would like to thank my wife and my family for their love, understanding, and every kind of support they provided not only throughout the thesis but also through my life.

Onur ŞAHİN

May, 2016

18/05/2016

**STATEMENT OF COMPLIANCE WITH ETHICAL PRINCIPLES
AND RULES**

I hereby truthfully declare that this thesis is an original work prepared by me; that I have behaved in accordance with the scientific ethical principles and rules throughout the stages of preparation, data collection, analysis and presentation of my work; that I have cited the sources of all the data and information that could be obtained within the scope of this study, and included these sources in the references section; and that this study has been scanned for plagiarism with “scientific plagiarism detection program” used by Anadolu University, and that “it does not have any plagiarism” whatsoever. I also declare that, if a case contrary to my declaration is detected in my work at any time, I hereby express my consent to all the ethical and legal consequences that are involved.

Onur ŞAHİN

TABLE OF CONTENTS

	<u>Page</u>
TITLE PAGE	i
APPROVAL OF JURY AND INSTITUTE	ii
ABSTRACT.....	iii
ÖZET	iv
ACKNOWLEDGMENTS.....	v
STATEMENT OF COMPLIANCE WITH ETHICAL PRINCIPLES AND RULES	vi
TABLE OF CONTENTS	vii
LIST OF FIGURES	ix
LIST OF ABBREVIATIONS	xi
1. INTRODUCTION	1
2. BACKGROUND	6
2.1 Fundamental Solution	6
2.1.1 Fundamental solution of the wave operator	8
2.1.2 Fundamental solution of the Laplace operator	9
2.2 Pseudo-Differential Operators	9
2.3 Poisson's Formula for the Half Space.....	11
2.4 Helmholtz Decomposition of a Vector Field	12
2.5 Equations of Elasticity	14
2.5.1 State of stress	14
2.5.2 State of strain.....	16
2.5.3 Stress-strain relations	17

	<u>Page</u>
2.5.4 Dynamic equations of motion	19
2.6 A Brief Account of Asymptotic Analysis	21
2.6.1 Watson's lemma	22
2.6.2 Laplace's method	23
2.6.3 Method of steepest descents	23
2.6.4 Method of stationary phase	24
2.7 Asymptotic Model for the Rayleigh Wave	25
3. 3-DIMENSIONAL MOVING LOAD PROBLEM FOR AN ELAS- TIC HALF-SPACE.....	28
3.1 Statement of the Problem	28
3.2 Near-Field Steady-State Solution	31
3.2.1 Super-Rayleigh case	32
3.2.2 Sub-Rayleigh case	38
3.3 Investigation of the Accuracy of the Asymptotic Solutions ...	47
3.4 Transient Surface Motion	50
3.5 Numerical Results of the Uncoated Half-Space	52
4. 3-DIMENSIONAL MOVING LOAD PROBLEM FOR A COATED ELASTIC HALF-SPACE.....	56
4.1 Statement of the Problem and Scaling	56
4.2 Solution of the Problem.....	59
4.2.1 Super-Rayleigh case	59
4.2.2 Sub-Rayleigh case	66
4.3 Numerical Results for the Coated Half-Space	71
5. CONCLUSIONS	76
REFERENCES	79
CURRICULUM VITAE	

LIST OF FIGURES

	<u>Page</u>
Figure 2.1. Components of stress.....	15
Figure 3.1. A load travelling along the surface of the half-space.....	28
Figure 3.2. Mach cone.....	30
Figure 3.3. Semicircular contour C for $\eta_2 > 0$	39
Figure 3.4. Semicircular contour C' for $\eta_2 < 0$	41
Figure 3.5. Keyhole contour with the poles $-\eta_1 + ik_1\eta_3$ and $-\eta_1 - ik_1\eta_3$. 43	43
Figure 3.6. Keyhole contour with the poles $\eta_1 + ik_1\eta_3$ and $\eta_1 - ik_1\eta_3$	45
Figure 3.7. Comparison of the derivatives of full and asymptotic solutions (3.57) and (3.74) in the sub-Rayleigh case, for $\nu = 0.25$, $\eta_1 = \eta_3 = 1$ and (a) $\varepsilon = 0.1$, (b) $\varepsilon = 0.01$	49
Figure 3.8. The scaled displacement U_3 vs. η_1 in the super-Rayleigh case for (a) $\eta_2 = 0$, (b) $\eta_2 = 1$	53
Figure 3.9. The scaled displacement U_3 vs. η_2 in the super-Rayleigh case for $\eta_1 = -1$	53
Figure 3.10. The scaled displacement U_1 vs. η_1 in the super-Rayleigh case for (a) $\eta_2 = 0$, (b) $\eta_2 = -1$	54
Figure 3.11. The scaled displacement U_3 vs. η_2 in the sub-Rayleigh case for $\eta_1 = 1$	55
Figure 4.1. Coated half-space under a moving load.	56
Figure 4.2. Asymptotic scaling.	59
Figure 4.3. Mach cone in coated half-space.....	65
Figure 4.4. Profile of the super-Rayleigh displacement U_1 at $ \xi = 5$	72
Figure 4.5. Profile of the super-Rayleigh displacement U_1 at $ \eta = 5$	73
Figure 4.6. A 3D profile of the longitudinal super-Rayleigh displacement U_1	73
Figure 4.7. Transverse cross-section of the sub-Rayleigh displacement profile U_1 at $ \eta = 5$	74

Figure 4.8. Longitudinal cross-section of the sub-Rayleigh displacement profile U_1 at $|\xi| = 10$ 74

Figure 4.9. A 3D profile of the longitudinal sub-Rayleigh displacement U_1 75



LIST OF ABBREVIATIONS

\mathbb{R}^n	: n-dimensional Euclidean space
\mathcal{D}	: Space of test function
\mathcal{D}'	: Space of generalized function
\square_a	: D'Alambert's operator
Δ	: Laplace's operator
$\delta(x)$: Dirac delta function
$H(x)$: Heaviside function
∇	: Gradient vector field
\mathbf{T}_n	: Traction
δ_{ij}	: Kronecker delta
σ_{ij}	: Components of stress
ε_{ij}	: Components of strain
λ, μ	: Lamé constants
E	: Young's modulus
ν	: Poisson's ratio
c_1	: Longitudinal wave speed
c_2	: Transverse wave speed
c_R	: Rayleigh wave speed
c	: Load speed
φ, ψ	: Wave potentials
O	: Big-O notation
o	: Little-O notation
ρ	: Volume density
$\sqrt{-\Delta_2}$: Pseudo-differential operator
$S(x), C(x)$: Fresnel functions
$Ai(z)$: Airy function

1. INTRODUCTION

The mathematical theory of elasticity is occupied with an attempt to reduce to calculation the state of strain, or relative displacement, within a solid body which is subject to the action of an equilibrating system of forces, or is a state of slight internal relative motion, and with endeavours to obtain results which shall be practically important in applications to architecture, engineering, and all other useful arts which the material of construction is solid, see [1].

The first consideration on the elasticity was carried out by Galileo in his work on the nature of the resistance of solid to rupture. In his work, Galileo endeavoured to determine the resistance of a beam, one end of which was fixed into a wall, when it is strained by its own weight or an applied load. This problem is called Galileo's problem. After Galileo's works on the beam attention of the mathematicians was directed to the Galileo's problem and several important researches on the elasticity were brought out by many scientists. But the most important discovery among of these researches was found out by Hooke in 1678. He stated that the stress imposed on a body is directly proportional to the strain produced so long as the limit of elasticity of body is not exceeded. This law is called Hooke's law, which constructs the basis of the mathematical theory of elasticity and is the first classical example of an explanation of elasticity. After the discovery of Hooke's law Navier's research on an elastic solid is to be regarded as the great landmark of the modern theory of elastic solids. Navier gave the first time the general equation of equilibrium and vibration of elastic solids in the case when the material was assumed to be isotropic and equation of equilibrium and vibration contained a single constant. Hence all questions about the displacement and the small strain of elastic bodies were reduced to a mathematical calculation. Cauchy introduced the notion of stress and showed that the stress, which is simply defined as the internal force neighbouring points exert on each other, can be indicated with the help of six component stresses, and also with the help of three purely normal tractions. This had brought a new perspective to mathematical theory of elasticity. He also showed that the state of strain near a point can be expressed in terms of six components. Cauchy obtained the equations of motion and equilibrium in terms of the displacements and expressed stress-strain

relation for isotropic materials. Cauchy's equations for motion differ from Navier's in one important respect. Navier's equations contains a single constant to express the elastic behaviour of a body, while Cauchy's definition contains two such constants. If we survey all progress in all the respects mentioned it can be observed that there are also a lot of great scientists that made significant contributions to the elasticity theory; Euler, Lagrange, Young, Poisson, Lamé to name but a few.

All research on the dynamical aspect of motion in elastic materials showed that the equations of the general theory of elasticity estimated that there are two kind of elastic waves which could propagate through an isotropic elastic solid. The first type of wave, called longitudinal or irrotational wave, is the faster one and propagates in the same direction as that of wave propagation. The second type of wave, called transverse or rotational wave, is the slower one and perpendicular to the propagation direction. These waves are called body waves since they act throughout the whole body. In 1885, however, Lord Rayleigh [2] considered waves propagating along the free surface of an isotropic homogeneous infinite elastic solid and investigated a third type of wave that could propagate along the surface. The velocity of waves of this type is less than that of either of the other two waves and the motion associated with the wave shows an exponential decay with distance into the material from the surface. This type of surface wave is now called Rayleigh wave. Rayleigh wave include both longitudinal and transverse waves and cause motion of the surface particles in an elliptical path which lies in a plane normal to surface and parallel to the direction of propagation. After Rayleigh's investigation surface waves became an important research area in linear elasticity. Another type of surface wave was later found by Love in 1911 (cf. [3]). This surface wave occurs in solids in which a surface layer of material is welded to the top of the solids and particle motion arise along a longitudinal line perpendicular to the direction of propagation. Love waves travel with a lower velocity than body waves, but faster than a Rayleigh wave. Due to the character of the surface waves Love waves also decay away from the surface. Yet another kind of wave propagating in an elastic solid is the Lamb wave which was investigated by Lamb in 1917 in his work on the wave motion in elastic plates (cf. [4]). Lamb showed that this kind of wave can be generated in a plate with free boundaries and particle motion lies in the plane containing the direction of wave propagation. In 20th cen-

tury similar types of waves were discovered among which are Stoneley waves which propagate along the boundary of two different elastic media in contact (cf. [5]). If one of the medium is a liquid then the corresponding wave is called a Scholte wave (cf. [6]).

Over the decades the surface waves have been investigated due to their applicability to acoustics, seismology, electromagnetism, among others and quite in-depth studies have been taken up in the last century. One of the important investigation among these researches on the Rayleigh wave was made by Friedlander [7]. In his work Friedlander considered the propagation of waves of arbitrary shape over the surface of a semi infinite elastic solid and showed that such a motion is possible only when the velocity of propagation is that of Rayleigh waves. Thus he presented a self similar solution of the homogeneous problem for an elastic half-plane in terms of arbitrary plane harmonic functions. In a later publication, Chadwick [8] analysed surface and interfacial waves of arbitrary form in isotropic, elastic media. He first extended Friedlander's solution and then demonstrated that this solution may be expressed in terms of a *single plane harmonic function* related to each other by means of a Hilbert transform. He also gave a relation between the wave potentials that provides a great convenience in obtaining the solution of the investigated problem when one of the potentials is determined. This relation, given in 2 dimensions, was then extended to 3 dimensions by Kiselev and Parker in their work: "Omni-directional Rayleigh, Stoneley and Schölte waves with general time dependence" [9].

Rayleigh wave does not appear explicitly in the general formulations of dynamical problems of the elasticity theory, which causes certain difficulties in the formulation of general theory of elastic waves. The significance of the Rayleigh wave on an elastic plane or space motivates an alternative analysis under more general assumptions, which can help to extract the Rayleigh wave contribution. Therefore recent studies have generally focused on deriving approximate models for Rayleigh waves. Knowles [10] was concerned with some generalizations of free harmonic Rayleigh waves and tried to acquire an approximate equation for free harmonic Rayleigh waves. Kaplunov and Kossovich [11] introduced an asymptotic model of Rayleigh waves in the far-field zone in elastic half space. This model makes possible to study dynamical effects associated with a Rayleigh wave field. Then in [12] the methodol-

ogy of [11] was extended to the Bleustein-Gulyaev surface wave and a 1-dimensional hyperbolic equation was derived for the surface shear deformation. Kaplunov et al. [13] reconsidered the problem formulated in [11] and [12] and presented an explicit model for the Rayleigh and Bleustein-Gulyaev surface waves. The derivations were based on perturbing in slow time the self-similar solution for homogeneous surface waves given in [7] and [8]. Thus the developed models for the two surface waves consisted of hyperbolic equation on the surface with elliptic equations in the interior domain. The formulation in [13] was later generalized to the 3-dimensional linear isotropic coated elastic half-space taking into account the effect of a thin coating, see [14]. The developed hyperbolic-elliptic model was also applied to a transient 2-dimensional moving load problem for an elastic half-plane in [15]. The problem was concerned with a near resonant regime in which the speed of the load is close to the Rayleigh wave speed.

Moving load problems have been analyzed for more than a century (see [16] and reference therein). Among the numerous studies that have been published on the subject, most of the contributions have been carried out within a 2-dimensional framework and only very few of them have focused on 3-dimensional framework. In spite of a distinct importance of 2-dimensional moving load problems, various modern industrial applications, including the development of high-speed train operations, include 3-dimensional modelling. The mathematical modelling of 3-dimensional problems in industrial applications motivates to focus on the numerical evaluation of exact solutions expressed in integral form. Georgiadis and Lykotrafitis [17] developed an integral transform procedure to obtain fundamental elastodynamic 3-dimensional solution for moving load over the surface of a half space by using the Radon transform that has been traditionally used to reduce the 3-dimensional problems to 2-dimensional ones in linear elasticity. Then the methodology developed in [17] and the hyperbolic-elliptic model in [13] were utilized for deriving a long wave model for a coated elastic half-space in [14].

The organization of the thesis is described as follows. After the Introduction given in Chapter 1, a brief account of the some basic definitions and concepts, frequently used throughout the thesis, are outlined in Chapter 2.

Chapter 3 starts with statement of the 3-dimensional moving load problem for

an uncoated half-space. The problem is formulated through the hyperbolic-elliptic model, derived in [13] and [14], and the steady-state equations of the motion on the surface for the sub and super-Rayleigh cases are presented. A steady-state analysis over the interior results in simple explicit expressions for the displacement components in the near-field of the point load steadily moving at a constant speed close to the Rayleigh wave one. Then a brief discussion of the transient surface response is given addressing, in particular, the resonant behaviour at the Rayleigh wave speed. Chapter 3 concludes with the illustrations of numerical results of the obtained asymptotic formulae and presents the accuracy of the asymptotics by comparison with the exact formulation.

In Chapter 4, 3-dimensional moving load problem for a coated half-space is considered. This chapter starts with statement of the problem, followed by the proposed asymptotic scaling. The sub and super-Rayleigh cases are analyzed and the solution for both cases, obtained through the use of integral transforms, are presented in terms of closed form integrals. Then the far-field asymptotic expansions of the integrals are obtained by employing approximate integration methods, uniform stationary phase method in particular. Numerical comparisons of exact and asymptotic results are presented for both cases and concluding remarks of the coated half-space problem are given.

Finally, in Chapter 5, conclusions are given and the main results of the thesis are discussed with suggestions for future work.

2. BACKGROUND

In this chapter some basic definitions and concepts, which are essential in the following chapters, are presented.

2.1. Fundamental Solution

Definition 2.1. A multi-index $\boldsymbol{\alpha} = (\alpha_1, \alpha_2, \dots, \alpha_n)$ is a vector whose components are nonnegative integers. The norm of a multi-index is defined by

$$|\boldsymbol{\alpha}| = \alpha_1 + \alpha_2 + \dots + \alpha_n, \quad (2.1)$$

and for any vector $\mathbf{x} = (x_1, x_2, \dots, x_n)$, multi-index power of a vector is defined as

$$\mathbf{x}^{\boldsymbol{\alpha}} = x_1^{\alpha_1} x_2^{\alpha_2} \dots x_n^{\alpha_n}. \quad (2.2)$$

Thus the multi-index power of a derivative operator $D^{\boldsymbol{\alpha}}$ is defined analogously

$$D^{\boldsymbol{\alpha}} = \frac{\partial^{|\boldsymbol{\alpha}|}}{\partial x_1^{\alpha_1} \partial x_2^{\alpha_2} \dots \partial x_n^{\alpha_n}}, \quad (2.3)$$

where $\boldsymbol{\alpha}$ is a multi-index and $\mathbf{x} = (x_1, x_2, \dots, x_n) \in \mathbb{R}^n$. This notation is highly convenient in writing partial differential operators.

Definition 2.2. Suppose that $f : \mathbf{X} \rightarrow \mathbb{R}^n$ is a real-valued function whose domain is an arbitrary set. The support of f is the set of points in \mathbf{X} where f is non-zero

$$\text{supp } f = \{\mathbf{x} \in \mathbf{X}; f(\mathbf{x}) \neq 0\}.$$

Definition 2.3. Let $\mathcal{D} = \mathcal{D}(\mathbb{R}^n)$ be the set of infinitely differentiable functions which have compact support in \mathbb{R}^n . The sequence of functions $\varphi_1, \varphi_2, \dots \in \mathcal{D}$ converges to the function φ (belonging to \mathcal{D}) if

- i. There is a number $R > 0$ such that $\text{supp } \varphi_k \subset U_R = \{x \in \mathbb{R}^n; |x| < R\}$,
- ii. For each $\boldsymbol{\alpha} = (\alpha_1, \alpha_2, \dots, \alpha_n)$, $D^{\boldsymbol{\alpha}} \varphi_k \rightrightarrows D^{\boldsymbol{\alpha}} \varphi$, $k \rightarrow \infty$.

Evidently \mathcal{D} is a linear space and this space is called the space of test functions, denoted, generally, by $\mathcal{D}(\mathbb{R}^n)$.

Definition 2.4. Each linear continuous functional over the space of test functions \mathcal{D} is called a generalized function and the set of all generalized functions is denoted by $\mathcal{D}' = \mathcal{D}'(\mathbb{R}^n)$. The effect of the generalized function f over the test function φ is denoted by (f, φ) .

Definition 2.5. The sequence of generalized functions $f_1, f_2, \dots \in \mathcal{D}'$ converges to $f \in \mathcal{D}'$ if, for any $\varphi \in \mathcal{D}$, $(f_k, \varphi) \rightarrow (f, \varphi)$ as $k \rightarrow \infty$. This is shown as $f_k \rightarrow f$ as $k \rightarrow \infty$ and called weak convergence.

Definition 2.6. The linear set \mathcal{D}' with the convergence defined in Definition 1.5 is known as the space of generalized functions \mathcal{D}' , see [18], [19].

Definition 2.7. Let α be a multi-index and L be an operator with coefficients $a_\alpha(\mathbf{x})$

$$L(\mathbf{x}, D) = L(D) = \sum_{|\alpha|=0}^m a_\alpha(\mathbf{x}) D^\alpha. \quad (2.4)$$

The generalized function $\mathcal{E} \in \mathcal{D}'$ which satisfies the equation

$$L(D)\mathcal{E} = \delta(x) \quad (2.5)$$

in \mathbb{R}^n is said to be the fundamental solution of the differential operator $L(D)$.

If $\mathcal{E}_0(x)$ is an arbitrary solution of the homogeneous equation $L(D)\mathcal{E}_0 = 0$, then the generalized function $\mathcal{E}(x) + \mathcal{E}_0(x)$ is also a fundamental solution of the operator $L(D)$:

$$L(D)(\mathcal{E} + \mathcal{E}_0) = L(D)\mathcal{E} + L(D)\mathcal{E}_0 = \delta(x).$$

Therefore the fundamental solution of an operator $L(D)$ is generally not unique. The main importance of the fundamental solution concept is that it helps to determine the solution of the non-homogenous differential equations. The following theorem shows how a solution of the non-homogenous equation can be obtained by using the fundamental solution.

Theorem 2.1. *Let $f \in \mathcal{D}'$ be such that the convolution of $\mathcal{E} * f$ exist in \mathcal{D}' . Then the solution of $L(D)u = f(x)$ exists in \mathcal{D}' and is given by the formula*

$$u = \mathcal{E} * f. \quad (2.6)$$

Proof. Since the convolution of $\mathcal{E} * f$ exist in \mathcal{D}' , it can be obtained from the properties of the convolution as

$$L(D)(\mathcal{E} * f) = (L(D)\mathcal{E}) * f = \delta * f = f. \quad (2.7)$$

Therefore the formula $u = \mathcal{E} * f$ gives the solution of non-homogenous differential equation. \square

In the following chapters we will make frequent use of fundamental solutions of some certain differential operators which now follows.

2.1.1. Fundamental solution of the wave operator

The first operator we consider is the wave operator (sometimes, called D'Alembert's operator) defined by

$$\square_a := \frac{\partial^2}{\partial t^2} - a^2 \Delta, \quad (2.8)$$

where Δ is Laplace's operator given by

$$\Delta = \frac{\partial^2}{\partial x_1^2} + \frac{\partial^2}{\partial x_2^2} + \cdots + \frac{\partial^2}{\partial x_n^2}. \quad (2.9)$$

The fundamental solution of the wave equation

$$\square_a \mathcal{E}_n = \delta(\mathbf{x}, t), \quad (2.10)$$

for $n = 1, 2, 3$ is given, respectively by

$$\mathcal{E}_1(x, t) = \frac{1}{2a} H(at - |x|), \quad (2.11)$$

$$\mathcal{E}_2(\mathbf{x}, t) = \frac{H(at - |\mathbf{x}|)}{2\pi a \sqrt{a^2 t^2 - |\mathbf{x}|^2}}, \quad (2.12)$$

and

$$\mathcal{E}_3(\mathbf{x}, t) = \frac{H(t)}{2\pi a} \delta(a^2 t^2 - |\mathbf{x}|^2), \quad (2.13)$$

where $H(x)$ is the Heaviside function. It is a common practise to write the wave operator in the form $\square_a = \Delta - \frac{1}{a^2} \frac{\partial^2}{\partial t^2}$ from which it follows that the fundamental solution of the wave equation for $n = 1$ becomes

$$\mathcal{E}(x, t) = \frac{a}{2} [H(x - at) - H(x + at)]. \quad (2.14)$$

2.1.2. Fundamental solution of the Laplace operator

The second operator we will encounter is the Laplace's operator defined by (2.9). The fundamental solution of the Laplace equation

$$\Delta \mathcal{E}_n = \delta(\mathbf{x}) \quad (2.15)$$

is given by

$$\mathcal{E}_n(\mathbf{x}) = \begin{cases} \frac{1}{2\pi} \ln |\mathbf{x}| & , \quad n = 2 \\ -\frac{|\mathbf{x}|^{2-n}}{(n-2)\omega_n} & , \quad n > 2, \end{cases} \quad (2.16)$$

where ω is the surface of unit sphere in \mathbb{R}^n , given with the formula

$$\omega_n = \frac{2\pi^{n/2}}{\Gamma(n/2)}.$$

2.2. Pseudo-Differential Operators

Pseudo-differential operators one of the interesting operators which play an important role when a differential operator has not constant but variable coefficients. Pseudo-differential operators are defined through the symbol of the differential operators considered the definition which we now give:

Definition 2.8. *Let α be a multi-index and $L(\mathbf{x}, D)$ be a differential operator given by equation (2.4). Then for any $\xi = (\xi_1, \xi_2, \dots, \xi_n) \in \mathbb{R}^n$ the symbol of $L(\mathbf{x}, D)$ is*

defined by

$$L(\mathbf{x}, i\boldsymbol{\xi}) = \sum_{|\boldsymbol{\alpha}| \leq m}^m a_{\boldsymbol{\alpha}}(\mathbf{x})(i\boldsymbol{\xi})^{\boldsymbol{\alpha}}. \quad (2.17)$$

The principal part of the symbol is

$$L^p(\mathbf{x}, i\boldsymbol{\xi}) = \sum_{|\boldsymbol{\alpha}|=m}^m a_{\boldsymbol{\alpha}}(\mathbf{x})(i\boldsymbol{\xi})^{\boldsymbol{\alpha}}. \quad (2.18)$$

For instance, the symbol of Laplace's operator is $-\xi_1^2 - \xi_2^2$, the symbol of the heat operator is $i\xi_1 + \xi_2^2$ and the symbol of the wave operator is $-\xi_1^2 + \xi_2^2$.

The Fourier inversion formula may be written as

$$f(\mathbf{x}) = \frac{1}{(2\pi)^n} \int \hat{f}(\boldsymbol{\xi}) e^{i\mathbf{x} \cdot \boldsymbol{\xi}} d\boldsymbol{\xi}, \quad (2.19)$$

where

$$\hat{f}(\boldsymbol{\xi}) = \frac{1}{(2\pi)^n} \int f(\mathbf{x}) e^{-i\mathbf{x} \cdot \boldsymbol{\xi}} d\mathbf{x} \quad (2.20)$$

is the Fourier transform of a function on \mathbb{R}^n . Differentiation of the inverse Fourier transform results in

$$D^{\boldsymbol{\alpha}} f(\mathbf{x}) = \frac{1}{(2\pi)^n} \int (i\boldsymbol{\xi})^{\boldsymbol{\alpha}} \hat{f}(\boldsymbol{\xi}) e^{i\mathbf{x} \cdot \boldsymbol{\xi}} d\boldsymbol{\xi}, \quad (2.21)$$

where $D^{\boldsymbol{\alpha}} = D_1^{\alpha_1} \dots D_n^{\alpha_n}$, $D_j = \partial/\partial x_j$. Hence, if the differential operator $L(\mathbf{x}, D)$ and its symbol are considered it can be obtained from equation (2.21)

$$L(\mathbf{x}, D)f(\mathbf{x}) = \frac{1}{(2\pi)^n} \int L(\mathbf{x}, i\boldsymbol{\xi}) \hat{f}(\boldsymbol{\xi}) e^{i\mathbf{x} \cdot \boldsymbol{\xi}} d\boldsymbol{\xi}. \quad (2.22)$$

Therefore it is seen that the Fourier transform of the differential operator $L(\mathbf{x}, D)$ acting on the function $f(\mathbf{x})$ is equal to the symbol of the operator multiplied by the Fourier transform of the function $f(\mathbf{x})$, i.e. $\hat{f}(\boldsymbol{\xi})$.

Definition 2.9. A differential operator $L(\mathbf{x}, D)$ on \mathbb{R}^n is an operator whose value on the function $f(\mathbf{x})$ is the function of x :

$$L(\mathbf{x}, D)f(\mathbf{x}) = \frac{1}{(2\pi)^n} \int L(\mathbf{x}, i\boldsymbol{\xi}) \hat{f}(\boldsymbol{\xi}) e^{i\mathbf{x} \cdot \boldsymbol{\xi}} d\boldsymbol{\xi},$$

where $\hat{f}(\boldsymbol{\xi})$ is the Fourier transform of $f(\mathbf{x})$ and $L(\mathbf{x}, i\boldsymbol{\xi})$ is the symbol of $L(\mathbf{x}, D)$. If $L(\mathbf{x}, i\boldsymbol{\xi})$ is an infinitely differentiable function on $\mathbb{R}^n \times \mathbb{R}^n$ with the property

$$|\partial_{\boldsymbol{\xi}}^{\boldsymbol{\alpha}} \partial_{\mathbf{x}}^{\boldsymbol{\beta}} L(\mathbf{x}, i\boldsymbol{\xi})| \leq C_{\boldsymbol{\alpha}, \boldsymbol{\beta}} (1 + |\boldsymbol{\xi}|)^{m - |\boldsymbol{\alpha}|}$$

for all $\mathbf{x}, \boldsymbol{\xi} \in \mathbb{R}^n$, all multi-indices $\boldsymbol{\alpha}, \boldsymbol{\beta}$, some constants $C_{\boldsymbol{\alpha}, \boldsymbol{\beta}}$ and some real number m , then L belongs to the symbol class consisting of C^∞ functions of slow growth. In this case the corresponding operator $L(\mathbf{x}, D)$ is called a pseudo differential operator of order m , see [20], [21].

2.3. Poisson's Formula for the Half Space

Definition 2.10. Let D be a domain in the space \mathbb{R}^n having a sufficiently smooth boundary S . The problem determining the solution of equation

$$\Delta u = 0, \tag{2.23}$$

with the boundary condition

$$\lim_{\mathbf{x} \rightarrow \mathbf{y}} u(\mathbf{x}) = \varphi(\mathbf{y}), \quad \mathbf{x} \in D, \quad \mathbf{y} \in S \tag{2.24}$$

is called the first boundary value problem or the Dirichlet problem. Here φ is a given real continuous function defined on S . The solution of the Dirichlet problem, $u(x)$, must be regular in the domain D and continuous in the closed region $D \cup S$.

Let us consider the case when the domain D is a half-space $x_n > 0$. Let \mathbf{x} and $\boldsymbol{\xi}$ be two points belonging to that half-space and let us take the point $\boldsymbol{\xi}' = (\xi_1, \xi_2, \dots, \xi_{n-1}, -\xi_n)$ symmetric with respect to the point $\boldsymbol{\xi}$ about the plane $\xi_n = 0$. If the boundary condition for the half-space $x_n > 0$ is given by

$$\lim_{\mathbf{x} \rightarrow \mathbf{y}} u(\mathbf{x}) = \varphi(y_1, y_2, \dots, y_{n-1}), \quad x_n > 0, \quad y_n = 0, \tag{2.25}$$

then the solution of the Dirichlet problem for the half-space becomes

$$u(\mathbf{x}) = \frac{\Gamma(n/2)}{\pi^{n/2}} x_n \int_{\xi_n=0} \frac{\varphi(\xi_1, \xi_2, \dots, \xi_{n-1})}{\left[\sum_{i=1}^{n-1} (\xi_i - x_i)^2 + x_n^2 \right]^{n/2}} d\xi_1 d\xi_2 \cdots d\xi_{n-1}, \quad (2.26)$$

where $\Gamma(n)$ is the gamma function. This formula is also called Poisson's formula, see [22].

2.4. Helmholtz Decomposition of a Vector Field

In writing the governing equations of motion of elasticity, it is a common practise represent the displacement field in terms of scalar and vector potentials. This is achieved through the application of Helmholtz decomposition of a vector.

Theorem 2.2. *Let $\mathbf{u}(\mathbf{x})$ be piecewise differentiable vector field in a finite open region V of \mathbb{R}^3 . Then $\mathbf{u}(\mathbf{x})$ can be decomposed into sum of gradient of a scalar and curl of a vector:*

$$\mathbf{u} = \nabla\varphi + \nabla \times \boldsymbol{\psi}. \quad (2.27)$$

This theorem is called the Helmholtz decomposition theorem.

Proof. Taking into account the properties of the Dirac delta function, the vector field $\mathbf{u}(\mathbf{x})$ can be represented as

$$\mathbf{u}(\mathbf{x}) = \int_V \mathbf{u}(\boldsymbol{\xi}) \delta(\mathbf{x} - \boldsymbol{\xi}) d\boldsymbol{\xi}. \quad (2.28)$$

It is also known from the Dirac delta function that

$$\delta(\mathbf{x} - \boldsymbol{\xi}) = -\frac{1}{4\pi} \nabla^2 \left(\frac{1}{|\mathbf{x} - \boldsymbol{\xi}|} \right). \quad (2.29)$$

Therefore equation (2.28) can be represented as

$$\mathbf{u}(\mathbf{x}) = -\frac{1}{4\pi} \nabla^2 \int_V \frac{\mathbf{u}(\boldsymbol{\xi})}{|\mathbf{x} - \boldsymbol{\xi}|} d\boldsymbol{\xi}. \quad (2.30)$$

On using the identity

$$\nabla^2 \mathbf{u} = \nabla (\nabla \cdot \mathbf{u}) - \nabla \times (\nabla \times \mathbf{u}), \quad (2.31)$$

equation (2.30) turns into

$$\mathbf{u} = -\frac{1}{4\pi} \nabla \left(\nabla \cdot \int_V \frac{\mathbf{u}(\boldsymbol{\xi})}{|\mathbf{x} - \boldsymbol{\xi}|} d\boldsymbol{\xi} \right) + \frac{1}{4\pi} \nabla \times \left(\nabla \times \int_V \frac{\mathbf{u}(\boldsymbol{\xi})}{|\mathbf{x} - \boldsymbol{\xi}|} d\boldsymbol{\xi} \right). \quad (2.32)$$

Thus the vector field $\mathbf{u}(\mathbf{x})$ is decomposed as

$$\mathbf{u} = \nabla \varphi + \nabla \times \boldsymbol{\psi}, \quad (2.33)$$

where

$$\varphi = -\frac{1}{4\pi} \nabla \cdot \int_V \frac{\mathbf{u}(\boldsymbol{\xi})}{|\mathbf{x} - \boldsymbol{\xi}|} d\boldsymbol{\xi}, \quad (2.34)$$

and

$$\boldsymbol{\psi} = \frac{1}{4\pi} \nabla \times \int_V \frac{\mathbf{u}(\boldsymbol{\xi})}{|\mathbf{x} - \boldsymbol{\xi}|} d\boldsymbol{\xi}, \quad (2.35)$$

see, [23]. □

This expression may also be written as

$$\mathbf{u} = \mathbf{u}_L + \mathbf{u}_T \quad (2.36)$$

where

$$\mathbf{u}_L = -\frac{1}{4\pi} \nabla \left(\nabla \cdot \int_V \frac{\mathbf{u}(\boldsymbol{\xi})}{|\mathbf{x} - \boldsymbol{\xi}|} d\boldsymbol{\xi} \right), \quad (2.37)$$

and

$$\mathbf{u}_T = \frac{1}{4\pi} \nabla \times \left(\nabla \times \int_V \frac{\mathbf{u}(\boldsymbol{\xi})}{|\mathbf{x} - \boldsymbol{\xi}|} d\boldsymbol{\xi} \right). \quad (2.38)$$

Since the curl of the gradient and the divergence of the curl are always vanishing it can be observed that \mathbf{u}_L is indeed a non-curling (longitudinal) vector field, $\nabla \times \mathbf{u}_L = 0$, whereas \mathbf{u}_T is indeed a non-divergence (transverse) vector field, $\nabla \cdot \mathbf{u}_T = 0$. Therefore the Helmholtz decomposition theorem also states that any well-behaved vector field can be decomposed into the sum of a longitudinal and a transverse vector field. Another point to be noted about the Helmholtz decomposi-

tion theorem is that the decomposition of a vector field given by equation (2.27) is generally not unique. Since the gradient of any constant and the curl of the gradient are zero, addition of such functions to φ and $\boldsymbol{\psi}$ respectively does not have any effect on equation (2.27). Thus there will be more than one equation which satisfy the Helmholtz decomposition. If it is also required that the field be outgoing at infinity, the uniqueness follows in that the constant and the gradient of the scalar function become zero. Under this assumption the Helmholtz decomposition of a vector field is uniquely determined by equation (2.27).

2.5. Equations of Elasticity

Elasticity is a property of solid materials which shows that how the materials are deformed under the action of applied external forces and resume their original shape and size after the force is removed. The theory of elasticity is a branch of continuum mechanics dealing with the elasticity of deformable bodies. This theory consists of a compatible set of equations which uniquely describe the state of stress, strain and displacements of each point with in elastic deformable body.

In this section we only mention some basic concepts and definitions of this comprehensive theory which will be used in the sequel.

2.5.1. State of stress

Definition 2.11. *Let us consider a body oriented by the unit normal \mathbf{n} with a number of forces acting on it. Taking an element with an area ΔA_n on the body and let the total force $\Delta \mathbf{F}_n$ acts on this small area. Then the stress vector or traction is defined as the limit of the ratio of the force vector to the surface area, i.e.,*

$$\lim_{\Delta A_n \rightarrow 0} \frac{\Delta \mathbf{F}_n}{\Delta A_n} = \frac{d\mathbf{F}_n}{dA_n} = \mathbf{T}_n. \quad (2.39)$$

In general, the stress vector can have any direction to the surface area ΔA_n . The vector \mathbf{T}_n may be regarded as the sum of two components that are normal and tangential to the surface element. Let us focus on an infinitesimal cubic element in order to find components of the stress vector acting on a particular object in a set of cartesian coordinates, see Figure 2.1. Here each axes of cartesian coordinates have

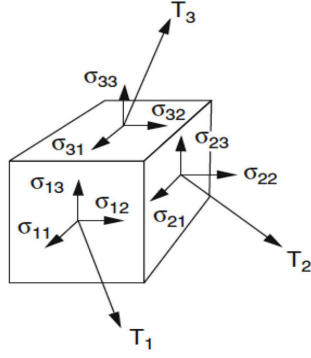


Figure 2.1. Components of stress.

a unit vector \mathbf{e}_i . As can be seen in Figure 2.1 the traction \mathbf{T}_i acts on each face i . Therefore each traction may be written in terms of its cartesian components in the form as

$$\mathbf{T}_i = \sigma_{ij}\mathbf{e}_j, \quad i, j = 1, 2, 3, \quad (2.40)$$

where a summation is assumed a repeating indices. Here the coefficients σ_{ij} are known as stresses and form a 3×3 matrix called the Cauchy stress tensor and shown as $\boldsymbol{\sigma}$;

$$\boldsymbol{\sigma} = \begin{pmatrix} \sigma_{11} & \sigma_{12} & \sigma_{13} \\ \sigma_{21} & \sigma_{22} & \sigma_{23} \\ \sigma_{31} & \sigma_{32} & \sigma_{33} \end{pmatrix}. \quad (2.41)$$

The first subscript i of the components of stress σ_{ij} refers to normal of the surface on which \mathbf{T}_i acts, and the second subscript j corresponds to direction of the stress \mathbf{T}_i . The component of the stress σ_{ii} is called the normal stress which is perpendicular to the surface, and σ_{ij} ($i \neq j$) is called the shear stress which is tangential to the surface. In some references, the normal and the shear stresses are shown as σ_i and τ_{ij} ($i \neq j$) respectively. However we will make use of the notation σ_{ii} and σ_{ij} ($i \neq j$) for the normal and shear stress throughout this thesis.

If the traction $\mathbf{T}_n = (T_i)$ acts on an arbitrary surface oriented by unit normal $\mathbf{n} = (n_i)$ then the traction can be expressed as

$$T_i = \sigma_{ji}n_j. \quad (2.42)$$

Thus the components of the stress vector for a cartesian coordinate or any surface

oriented by a unit normal \mathbf{n} can be expressed in terms of the components of the Cauchy stress tensor.

2.5.2. State of strain

Definition 2.12. *The relative change in the position of points in the body that has undergone deformation due to external or internal forces is called strain and shown as ε . The strain, ε , of a material line element is expressed as the change in the length Δl per unit of the original length l of the line element;*

$$\varepsilon = \frac{\Delta l}{l}. \quad (2.43)$$

The strain is positive if the object is stretched and negative if the object is compressed. As can be seen from the definition of the strain, unlike stress, strain is a dimensionless expression.

Strain may also be classified as normal and shear strains. Normal strain measures changes in length along a specific direction due to an applied force. It is also called extensional strain or dimensional strain and shown as ε_{ii} . So ε_{11} is the relative elongation or contraction of the length of the material along the x_1 axis. Shear strain measures changes in angle with respect to two specific directions. It is shown as ε_{ij} ($i \neq j$). As an example, ε_{12} gives the angular change between the x_1 and x_2 axes. The normal and the shear strains, in literature, are sometimes shown as σ_i and γ_{ij} ($i \neq j$) respectively. However we will use σ_{ii} and σ_{ij} ($i \neq j$) for the normal and shear stress respectively.

Let the component of a vector field $\mathbf{u}(\mathbf{x})$ be denoted by $u_i(x_1, x_2, x_3)$. If the functions $u_i(x_1, \dots, x_n)$ are differentiable then the partial derivatives of the displacement may be denoted by the indicial notation as $u_{i,j} = \partial u_i / \partial x_j$. Hence the infinitesimal strain-displacement relationships can be given with the indicial notation as

$$\varepsilon_{ij} = \frac{1}{2} (u_{i,j} + u_{j,i}). \quad (2.44)$$

2.5.3. Stress-strain relations

The most famous and elementary relation of the material behaviour is Hooke's law which states that deformation of the elastic material is proportional to applied force. This can be expressed mathematically as

$$F = kx, \tag{2.45}$$

where F is the force applied to the material and x is the displacement. Since stress is a force and strain is a displacement, the stresses and strains of the materials are connected by a *linearized* relationship that is mathematically similar to Hooke's law, and is often referred to by the same name. Therefore in one dimension, the relation between the stress and strain can be presented as

$$\sigma_{11} = E \varepsilon_{11}, \tag{2.46}$$

where E is called modulus of elasticity or Young's modulus. In general, Hooke's law, relating the stress tensor to the strain, is written in the form of a fourth-order tensor as

$$\sigma_{ij} = E_{ijkl} \varepsilon_{kl}, \tag{2.47}$$

where the 81 coefficients E_{ijkl} are called elastic constants. Taking into account certain material and geometric properties (symmetry, etc) of the elastic medium as well as symmetry of the stress tensor, the number of elastic constants reduce to 21. A material exhibiting different properties in different directions is called anisotropic. In the anisotropic materials these coefficients cannot be reduced any further. Therefore it will be first assumed that the material is independent from any directions. In this case number of the elastic constants is reduced to 9 producing an orthotropic material which has 3 mutually orthogonal planes of elastic symmetry. Finally for an additional simplification, directional and rotational independence is assumed. This assumption reduces the number of the constants to 2 producing an isotropic material which has uniform physical properties in all orientations. Thus

the relation between the stress and strain can be written as

$$\sigma_{ij} = \lambda \varepsilon_{kk} \delta_{ij} + 2\mu \varepsilon_{ij}, \quad (2.48)$$

where λ and μ are known as Lamé constants and δ_{ij} is Kronecker delta. If the strain-displacement relations given by equation (2.44) are substituted into the above equality, stress-displacement relations is written as

$$\sigma_{ij} = \lambda u_{k,k} \delta_{ij} + \mu (u_{i,j} + u_{j,i}), \quad (2.49)$$

see [24]. If these relations are written in an explicit form, we have for $i = 1, 2$, $j = 1, 2$ ($i \neq j$), and $k = 1, 2, 3$

$$\sigma_{ij} = \mu \left(\frac{\partial u_i}{\partial x_j} + \frac{\partial u_j}{\partial x_i} \right), \quad \sigma_{ii} = (\lambda + 2\mu) \frac{\partial u_i}{\partial x_i} + \lambda \left(\frac{\partial u_j}{\partial x_j} + \frac{\partial u_3}{\partial x_3} \right), \quad (2.50)$$

$$\sigma_{3i} = \sigma_{i3} = \mu \left(\frac{\partial u_i}{\partial x_3} + \frac{\partial u_3}{\partial x_i} \right), \quad \sigma_{33} = \lambda \left(\frac{\partial u_i}{\partial x_i} + \frac{\partial u_j}{\partial x_j} \right) + (\lambda + 2\mu) \frac{\partial u_3}{\partial x_3}.$$

It is also known from Hooke's law that the relation between the stress and strain in one dimension can be expressed by equation (2.46). Therefore if equation (2.46) is substituted into equation (2.48), the following equality is obtained.

$$\sigma_{11} = \frac{\mu(3\lambda + 2\mu)}{\mu + \lambda} \varepsilon_{11}. \quad (2.51)$$

This equality gives us Young's modulus, E , in terms of the Lamé constants as

$$E = \frac{\mu(3\lambda + 2\mu)}{\mu + \lambda}. \quad (2.52)$$

Another important elastic coefficient different from aforementioned coefficients is Poisson's ratio ν . Poisson's ratio is the negative ratio of transverse strain to the axial strain in the direction of the applied load. When a load is applied to a material, the material tends to expand or contract in the other two directions perpendicular to the direction of the load. This transverse change will bear a fixed relationship to the axial strain. The relationship, or ratio, of the transverse strain is called Poisson's

ratio. If the subscript 1 corresponds to the axial direction and subscripts 2 and 3 correspond to the transverse directions then Poisson's ratio can be written as

$$\nu = -\frac{\varepsilon_{22}}{\varepsilon_{11}} = -\frac{\varepsilon_{33}}{\varepsilon_{11}} = \frac{\lambda}{2(\mu + \lambda)}. \quad (2.53)$$

Since λ must remain finite, Poisson's ratio lies between $-1 < \nu < 0.5$.

2.5.4. Dynamic equations of motion

Let us consider a body occupying a regular region V in space with boundary S . The surface S is subjected to a distribution of surface traction \mathbf{T} and each mass element of the body may be subjected to a body force per unit mass, \mathbf{f} . Then the system of equations of equilibrium of a homogenous, isotropic, linear elastic body may be obtained from the principle of linear momentum as

$$\sigma_{ji,j} + \rho f_i = \rho \ddot{u}_i, \quad (2.54)$$

where u_i is the components of the displacement and ρ is the mass density. If the stress-displacement (2.49) are substituted into equation (2.54), displacement equations of motion are determined as

$$\mu u_{i,jj} + (\lambda + \mu) u_{j,ji} + \rho f_i = \rho \ddot{u}_i. \quad (2.55)$$

These equations are called Navier equations and they can be expressed in vector notation as

$$\mu \nabla^2 \mathbf{u} + (\lambda + \mu) \nabla \nabla \cdot \mathbf{u} + \rho \mathbf{f} = \rho \ddot{\mathbf{u}}. \quad (2.56)$$

In cartesian coordinates, where the displacements and the body mass are denoted by $\mathbf{u} = (u_1, u_2, u_3)$ and $\mathbf{f} = (f_1, f_2, f_3)$ respectively, Navier equations can be written

in an explicit form as

$$\begin{aligned}
(\lambda + \mu) \left(\frac{\partial^2 u_1}{\partial x^2} + \frac{\partial^2 u_2}{\partial x \partial y} + \frac{\partial^2 u_3}{\partial x \partial z} \right) + \mu \nabla^2 u_1 + \rho f_1 &= \rho \frac{\partial^2 u_1}{\partial t^2}, \\
(\lambda + \mu) \left(\frac{\partial^2 u_2}{\partial y \partial x} + \frac{\partial^2 u_2}{\partial y^2} + \frac{\partial^2 u_3}{\partial y \partial z} \right) + \mu \nabla^2 u_2 + \rho f_2 &= \rho \frac{\partial^2 u_2}{\partial t^2}, \\
(\lambda + \mu) \left(\frac{\partial^2 u_1}{\partial z \partial x} + \frac{\partial^2 u_2}{\partial z \partial y} + \frac{\partial^2 u_3}{\partial z^2} \right) + \mu \nabla^2 u_3 + \rho f_3 &= \rho \frac{\partial^2 u_3}{\partial t^2}.
\end{aligned} \tag{2.57}$$

We know from the Helmholtz decomposition of the a vector that any vector can be written sum of the gradient of a scalar and the curl of a vector. Therefore the displacement \mathbf{u} and the body mass \mathbf{f} can be written as

$$\mathbf{u} = \nabla \varphi + \nabla \times \boldsymbol{\psi}, \tag{2.58}$$

and

$$\mathbf{f} = c_1^2 \nabla F + c_2^2 \nabla \times \mathbf{G}, \tag{2.59}$$

where φ and $\boldsymbol{\psi}$ are scalar and vector potentials and c_1 and c_2 are longitudinal and transverse wave speeds given by

$$c_1^2 = \frac{\lambda + 2\mu}{\rho} \quad \text{and} \quad c_2^2 = \frac{\mu}{\rho}, \tag{2.60}$$

respectively. Substituting equations (2.58) and (2.59) into equation (2.56) gives the following non-homogenous wave equations.

$$\nabla^2 \varphi + F = \frac{1}{c_1^2} \ddot{\varphi}, \tag{2.61}$$

$$\nabla^2 \boldsymbol{\psi} + \mathbf{G} = \frac{1}{c_2^2} \ddot{\boldsymbol{\psi}}. \tag{2.62}$$

In the absence of body forces these equations turn to

$$\nabla^2 \varphi = \frac{1}{c_1^2} \ddot{\varphi}, \tag{2.63}$$

$$\nabla^2 \boldsymbol{\psi} = \frac{1}{c_2^2} \ddot{\boldsymbol{\psi}}. \tag{2.64}$$

homogenous wave equations, see [25].

2.6. A Brief Account of Asymptotic Analysis

Asymptotic analysis is an important field in applied analysis which is concerned with the determination of the behaviour of a function or obtaining approximate analytical solution of problems of differentiation and integration as one of its parameters becomes either very large or very small. Asymptotic analysis have found extensive use in obtaining of approximate solutions of some problems which may not be analytically solved in the areas of, say, fluid mechanics, difference equations, diffraction theory, number theory, etc.

We now give some basic notations and some useful techniques for finding approximate solutions of some certain integrals.

Definition 2.13. *Let $f(z)$ and $g(z)$ be two functions defined on D . Then we write*

$$f(z) = O(g(z)), \quad \text{as } z \rightarrow z_0 \quad (2.65)$$

if we can find a constant $K > 0$ and a neighbourhood U of z_0 so that

$$|f(z)| \leq K |g(z)|, \quad z \in D \cap U. \quad (2.66)$$

This means that f is bounded in a magnitude by a fixed multiple of g for all $z \in D \cap U$. If $f(z)$ and $g(z)$ are such that, for any given $\varepsilon > 0$ there exists a neighbourhood U_ε of z_0 so that

$$|f(z)| \leq \varepsilon |g(z)|, \quad z \in D \cap U_\varepsilon, \quad (2.67)$$

we say

$$f(z) = o(g(z)), \quad \text{as } z \rightarrow z_0. \quad (2.68)$$

This means that f is smaller in a magnitude than any multiple of g for all $z \in D \cap U_\varepsilon$ close enough to z_0 .

If $f(z)/g(z)$ tends to unity as $z \rightarrow z_0$, then we write

$$f(z) \sim g(z), \quad \text{as } z \rightarrow z_0. \quad (2.69)$$

and say that f and g are asymptotically equal.

Definition 2.14. A sequence of function $\varphi_n(z) \in D$ is called an asymptotic sequence as $z \rightarrow z_0$ from D if for all $n \geq 0$ we have

$$\varphi_{n+1}(z) = o(\varphi_n(z)), \quad \text{as } z \rightarrow z_0. \quad (2.70)$$

Then

$$\sum_{n=0}^N a_n \varphi_n(z)$$

is called an asymptotic expansion or an asymptotic approximation of the function $f(z)$ if for each N

$$f(z) = \sum_{n=0}^N a_n \varphi_n(z) + o(\varphi_N(z)), \quad \text{as } z \rightarrow z_0, \quad (2.71)$$

where a_n are constants. Thus it can be written

$$f(z) \sim \sum_{n=0}^{\infty} a_n \varphi_n(z), \quad \text{as } z \rightarrow z_0. \quad (2.72)$$

2.6.1. Watson's lemma

Suppose $\phi(t)$ is a complex valued, absolutely integrable function on $[0, T]$

$$\int_0^T |\phi(t)| dt < \infty.$$

Suppose also that $\phi(t)$ is of the form $\phi(t) = t^\sigma g(t)$ where $\sigma > -1$ and $g(t)$ is a function which possesses a Taylor expansion around $t = 0$ with $g(0) \neq 0$. Then the exponential integral

$$F(\lambda) = \int_0^{\infty} e^{-\lambda t} \phi(t) dt \quad (2.73)$$

is finite for all $\lambda > 0$ and has the asymptotic expansion

$$F(\lambda) \sim \sum_{n=0}^T \frac{g^{(n)}(0) \Gamma(\sigma + n + 1)}{n! \lambda^{\sigma + n + 1}}, \quad \text{as } \lambda \rightarrow \infty, \quad (2.74)$$

see [26].

2.6.2. Laplace's method

Laplace's method considers integrals of the type

$$F(\lambda) = \int_{\alpha}^{\beta} g(t)e^{\lambda h(t)} dt, \quad (2.75)$$

where λ is real and positive, $g(t)$ is a real continuous function and $h(t)$, $h'(t)$ and $h''(t)$ are real and continuous functions in $\alpha \leq t \leq \beta$ and the range of the integration may be finite or infinite. According to Laplace's idea the major contribution to these type of integrals, as $\lambda \rightarrow \infty$, comes from the neighbourhood of the point in $\alpha \leq t \leq \beta$ where $h(t)$ has its maximum value. Therefore if $h(t)$ has its maximum value at a point $\gamma \in (\alpha, \beta)$, then $h'(\gamma) = 0$ and $h''(\gamma) \neq 0$ and the asymptotic expansion of the integral given by (2.75) may be written as

$$F(\lambda) \sim g(\gamma) \left\{ \frac{-\pi}{2\lambda h''(\gamma)} \right\}^{1/2} e^{\lambda h(\gamma)}, \quad \lambda \rightarrow \infty. \quad (2.76)$$

If $h(t)$ has its maximum value at one of the end points $t = \alpha$ or $t = \beta$, the asymptotic expansions take the forms

$$F(\lambda) \sim \left\{ \frac{-g(\alpha)}{\lambda h''(\alpha)} \right\}^{1/2} e^{\lambda h(\alpha)}, \quad \lambda \rightarrow \infty, \quad (2.77)$$

and

$$F(\lambda) \sim \left\{ \frac{g(\beta)}{\lambda h''(\beta)} \right\}^{1/2} e^{\lambda h(\beta)}, \quad \lambda \rightarrow \infty. \quad (2.78)$$

respectively, see [27].

2.6.3. Method of steepest descents

The method of steepest descents is a generalization of Laplace's method that is adapted to certain types of exponential integrals of the form

$$F(\lambda) = \int_C g(z)e^{\lambda h(z)} dz, \quad (2.79)$$

where C is some contour in the complex plane, $g(z)$ and $h(z)$, which are independent of λ , are analytic functions of z in some domain of the complex plane which contains the contour C , and λ is a real positive parameter. The problem is to find an asymptotic approximation of $F(\lambda)$ for large λ . Since $h(z)$ is a complex valued function it can be written as $h(z) = \phi + i\psi$. Therefore imaginary part ψ of $h(z)$ gives an oscillatory contribution $e^{i\lambda\psi}$ to the integrand. This method is basically based on choosing a contour which reduces the effect of the oscillations so that the contour passes through the point $z = z_0$ where real part ϕ of $h(z)$ has its maximum value on it. This specific contour is called steepest descent path. On the steepest descent path since there are no oscillations from $e^{i\lambda\psi}$ and $e^{\lambda\phi}$ has its maximum value at z_0 on the path, the asymptotic expansion of the integral (2.79) can be obtained from the Laplace's method as

$$F(\lambda) \sim g(z_0) \left\{ \frac{-2\pi}{\lambda h''(z_0)} \right\}^{1/2} e^{\lambda h(z_0)}, \quad \text{as } \lambda \rightarrow \infty. \quad (2.80)$$

2.6.4. Method of stationary phase

This is a method for deriving asymptotic expansion of integrals of the form

$$F(\lambda) = \int_a^b g(t) e^{i\lambda h(t)} dt, \quad (2.81)$$

where a , b , $g(t)$, $h(t)$ and t are real and λ is a large real parameter. Since the term $e^{i\lambda h(t)}$ only gives oscillations the aforementioned methods, Watson's lemma, Laplace's method or steepest descent method, cannot be used due to the absence of exponential decay of the integrands. If λ is large, the rapid oscillations caused by the factor $e^{i\lambda h(t)}$ will be very dense so there will be cancellations of positive and negative parts of the oscillation almost everywhere except for some points which make the function $h(t)$ zero. These points are called stationary points. Therefore it is safe to assume that the main contribution to the integral comes from a neighbourhood of the stationary points, or the end points of the integral. This is the basic idea behind of method of stationary phase. Thus, when the function $h(t)$ has only one stationary point $t_0 \in (a, b)$, the asymptotic expansion of the integral $F(\lambda)$ in (2.81)

as $\lambda \rightarrow \infty$ is given by

$$F(\lambda) \sim g(t_0) \left\{ \frac{2\pi}{\lambda |h''(t_0)|} \right\}^{1/2} e^{i(\lambda h(t_0) \pm \pi/4)}, \quad \lambda \rightarrow \infty, \quad (2.82)$$

where the positive and negative signs in the exponential correspond $h''(t_0) > 0$ and $h''(t_0) < 0$ respectively. When there is more than one stationary point of the function $h(t)$ the asymptotic expansion of integral (2.81) may be given by summing of the contributions of the each stationary points.

If $h(t)$ does not have any stationary points in (a, b) then the only contribution to the integral comes from the end points $t = a$ and $t = b$ as $\lambda \rightarrow \infty$. Thus the asymptotic expansion of the integral can be obtained as

$$F(\lambda) \sim \frac{1}{\lambda} \left\{ \frac{g(b)}{ih'(b)} e^{i\lambda h(b)} - \frac{g(a)}{ih'(a)} e^{i\lambda h(a)} \right\}, \quad \lambda \rightarrow \infty. \quad (2.83)$$

2.7. Asymptotic Model for the Rayleigh Wave

The analysis of 3D moving load problems for uncoated and coated elastic half-spaces, which is the main subject of this thesis, are based on the hyperbolic-elliptic asymptotic model developed by Kaplunov et al. [13] and also presented by Dai et al. in [14]. The model is aimed at obtaining the Rayleigh wave contribution of the overall dynamic response of the elastic medium ignoring the effects of bulk waves, and in turn provides a simpler analysis of the considered problems. Since we generalize this method to 3D problems it is best to give a short account here.

In [13], Kaplunov et al. considered a stationary load problem for an elastic half plane with the boundary condition at $y = 0$ given by

$$\sigma_{22}(x, 0, t) = -P_1(x, t), \quad (2.84)$$

and investigated solution of the governing equations of the motion

$$\frac{\partial^2 \phi}{\partial x^2} + \frac{\partial^2 \phi}{\partial y^2} - \frac{1}{c_1^2} \frac{\partial^2 \phi}{\partial t^2} = 0, \quad \frac{\partial^2 \psi}{\partial x^2} + \frac{\partial^2 \psi}{\partial y^2} - \frac{1}{c_1^2} \frac{\partial^2 \psi}{\partial t^2} = 0, \quad (2.85)$$

in dimensionless form given by

$$\begin{aligned}\phi &= \frac{P_*}{\varepsilon\mu} (\phi_0(\xi, y, \tau) + \varepsilon\phi_1(\xi, y, \tau) + \dots), \\ \psi &= \frac{P_*}{\varepsilon\mu} (\psi_0(\xi, y, \tau) + \varepsilon\psi_1(\xi, y, \tau) + \dots),\end{aligned}\tag{2.86}$$

where c_R is the Rayleigh wave speed, $\xi = x - c_R t$, $\tau = \varepsilon t$ ($\varepsilon \ll 1$) and $P_* = \max_{(x,t)} = (P_1(x, t))$. Substituting of the asymptotic expansions (2.86) into the equations of the motion and taking into account the leading order terms give the following elliptic equations in the interior of the half-plane

$$\begin{aligned}\frac{\partial^2 \phi}{\partial y^2} + k_1^2 \frac{\partial^2 \phi}{\partial x^2} &= 0, \\ \frac{\partial^2 \psi}{\partial y^2} + k_2^2 \frac{\partial^2 \psi}{\partial x^2} &= 0.\end{aligned}\tag{2.87}$$

Applying the same process to the boundary condition results in

$$\frac{\partial^2 \phi}{\partial x^2} - \frac{1}{c_R^2} \frac{\partial^2 \phi}{\partial t^2} = AP_1,\tag{2.88}$$

where

$$k_i^2 = 1 - \frac{c_R^2}{c_i^2}, \quad (i = 1, 2),\tag{2.89}$$

and A is a material constant given by

$$A = \frac{k_1 k_2 (1 + k_2^2)}{2\mu [k_2^2 (1 - k_1^2) + k_1^2 (1 - k_2^2) - k_1 k_2 (1 - k_2^4)]}.\tag{2.90}$$

Besides, the second potential ψ can be found from the boundary condition as

$$\frac{\partial \psi}{\partial x} = -\frac{2}{1 + k_2^2} \frac{\partial \phi}{\partial y}, \quad \text{at } y = 0.\tag{2.91}$$

This equation, which was first introduced by Chadwick [8], shows that the wave potentials are related to each other by means of a Hilbert transform.

In [14], Dai et al. dealt with the 3D stationary load problem for a linear isotropic elastic coated half-space. The coating was modelled via the effective boundary conditions on the surface of the substrate and the effect of the boundary condition

under the coating was estimated. Then the problem was reduced to a 2D problem through the Radon transform that has been generally used for reduction of the 3D to 2D ones in linear elasticity. Thus the problem was reduced in a form where it was possible to implement to explicit model introduced in [13], which gives two 2D elliptic equations over the interior and a hyperbolic equation on the surface. As the asymptotic solution was obtained through the model, by inverting the obtained equations to the original variables the 3D model, in the end, was expressed through the 3D elliptic equations in the interior ($x_3 > h$)

$$\begin{aligned}\frac{\partial^2 \phi}{\partial x_3^2} + k_1^2 \Delta_2 \phi &= 0, \\ \frac{\partial^2 \psi_i}{\partial x_3^2} + k_2^2 \Delta_2 \psi_i &= 0, \quad (i = 1, 2)\end{aligned}\tag{2.92}$$

with 2D hyperbolic equation singularly perturbed by a pseudo-differential operator on the surface

$$\Delta_2 \phi - \frac{1}{c_R^2} \frac{\partial^2 \phi}{\partial t^2} + \frac{bh}{k_1} \frac{\partial}{\partial x_3} (\Delta_2 \phi) = AP, \quad \text{at } x_3 = h,\tag{2.93}$$

and relation with the potentials

$$\frac{\partial \psi_i}{\partial x_3} = \frac{2}{1 + k_2^2} \frac{\partial \phi}{\partial x_i}, \quad (i = 1, 2), \quad \text{at } x_3 = h,\tag{2.94}$$

where $\boldsymbol{\psi} = (-\psi_2, \psi_1, 0)$. Unlike the surface equation of the uncoated half-plane problem in [13], the surface equation given by (2.93) contains a singular perturbation in the form of a pseudo-differential operator.

Both models for uncoated and coated half spaces are quite useful to reduce the 2D and 3D vector problems to a scalar problems. Moreover the relation between the potentials enables to find each of the potentials without lengthy calculations when one of the potentials is determined.

3. 3-DIMENSIONAL MOVING LOAD PROBLEM FOR AN ELASTIC HALF-SPACE

In this chapter we will investigate the 3D dynamic response of an elastic half-space loaded by a vertical point force moving along a straight line on the surface of the elastic half-space at a constant speed which is assumed to be close to the Rayleigh wave speed. This problem will be formulated within the framework of the asymptotic hyperbolic-elliptic model developed in [13] and [14] and steady state equations of the motion will be presented through the asymptotic model. Finally in order to verify the accuracy of the approximate solution, comparisons of the asymptotic and exact results will be illustrated.

3.1. Statement of the Problem

We consider a linear elastic isotropic half-space occupying the region $-\infty < x_1, x_2 < \infty, 0 \leq x_3$. The equations of motion in 3D elasticity are given by (see [23])

$$(c_1^2 - c_2^2)\text{grad div } \mathbf{u} + c_2^2\Delta\mathbf{u} = \mathbf{u}_{tt}, \quad (3.1)$$

where Δ is 3D Laplace operator, $\mathbf{u} = (u_1, u_2, u_3)$ is the displacement vector, t is time, and c_1 and c_2 are the longitudinal and transverse wave speeds, given by (2.60), respectively. Here, a vertical point force of amplitude P is applied on the boundary of the elastic half-space and this force is moving at a constant speed c along the Ox_1 axis, see Figure 3.1. Therefore the boundary condition on the surface $x_3 = 0$ may

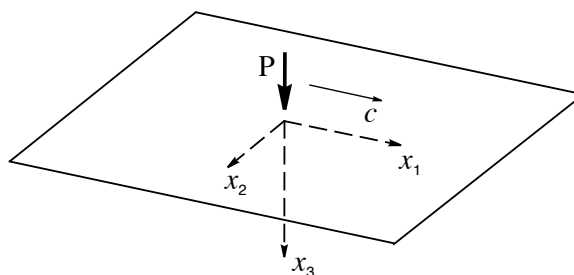


Figure 3.1. A load travelling along the surface of the half-space.

be written as (cf. eqn. (2.50))

$$\frac{\partial u_3}{\partial x_i} + \frac{\partial u_i}{\partial x_3} = 0, \quad (i = 1, 2), \quad (3.2)$$

$$(c_1^2 - 2c_2^2) \left(\frac{\partial u_1}{\partial x_1} + \frac{\partial u_2}{\partial x_2} \right) + c_1^2 \frac{\partial u_3}{\partial x_3} = \frac{P}{\rho} \delta(x_1 - ct) \delta(x_2), \quad (3.3)$$

where ρ is the volume density.

Instead of the conventional setup (3.1), (3.2) and (3.3), we start from the 3D hyperbolic-elliptic approximate formulation given in [13], [14], oriented to extraction of the Rayleigh wave contribution to the overall dynamic response. Therefore we have the following elliptic equation in the interior

$$\frac{\partial^2 \varphi}{\partial x_3^2} + k_1^2 \Delta_2 \varphi = 0, \quad \frac{\partial^2 \psi_i}{\partial x_3^2} + k_2^2 \Delta_2 \psi_i = 0, \quad (i = 1, 2), \quad (3.4)$$

and 2D hyperbolic equation along the surface $x_3 = 0$

$$\Delta_2 \varphi - \frac{1}{c_R^2} \frac{\partial^2 \varphi}{\partial t^2} = AP \delta(x_1 - ct) \delta(x_2), \quad (3.5)$$

along with the relations

$$\frac{\partial \varphi}{\partial x_i} = \frac{2}{1 + k_2^2} \frac{\partial \psi_i}{\partial x_3}, \quad (i = 1, 2), \quad (3.6)$$

where $\Delta_2 = \partial^2 / \partial x_1^2 + \partial^2 / \partial x_2^2$ is the 2D Laplace operator and k_i and A are defined by equations (2.89) and (2.90) respectively.

Throughout this problem we mainly deal with a steady-state limit in which the type of equation (3.5), rewritten in terms of the moving coordinate $\lambda = x_1 - ct$, depends on the load speed c . Thus we get from equation (3.5)

$$\frac{\partial^2 \varphi}{\partial x_2^2} + \left(1 - \frac{c^2}{c_R^2} \right) \frac{\partial^2 \varphi}{\partial \lambda^2} = AP \delta(\lambda) \delta(x_2). \quad (3.7)$$

Equation (3.7) signifies that the type of the boundary equation, i.e. it being elliptic or hyperbolic depends on the load speed c being less than or greater than the Rayleigh

wave speed c_R . Introducing the dimensionless parameter

$$\varepsilon = \sqrt{\left|1 - \frac{c^2}{c_R^2}\right|}, \quad (3.8)$$

equation (3.7) reduces to the hyperbolic equation

$$\frac{\partial^2 \varphi}{\partial x_2^2} - \varepsilon^2 \frac{\partial^2 \varphi}{\partial \lambda^2} = AP\delta(\lambda)\delta(x_2), \quad (3.9)$$

in the super-Rayleigh case ($c > c_R$) and to the elliptic equation

$$\frac{\partial^2 \varphi}{\partial x_2^2} + \varepsilon^2 \frac{\partial^2 \varphi}{\partial \lambda^2} = AP\delta(\lambda)\delta(x_2), \quad (3.10)$$

in the sub-Rayleigh case ($c < c_R$). We thus observe a drastic distinction between the 3D sub and super-Rayleigh cases which is not a feature of the plane strain moving load problem (cf. [29]). In particular, now we have a Mach cone associated with the hyperbolic equation (3.9), see Figure 3.2.

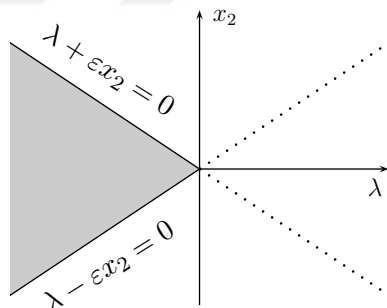


Figure 3.2. Mach cone.

The adapted approximation is valid provided that $\varepsilon \ll 1$, i.e. when the speed of the load is close to the Rayleigh wave speed. The presence of the small physical parameter in equations (3.9) and (3.10) motivates a near-field asymptotic analysis. On introducing scaled variables by

$$\eta_1 = \frac{\lambda}{\varepsilon}, \quad \eta_2 = x_2, \quad \eta_3 = \frac{x_3}{\varepsilon}, \quad (3.11)$$

we rewrite equations (3.4), (3.9), (3.10) and (3.6), having

$$\frac{\partial^2 \varphi}{\partial \eta_3^2} + k_1^2 \frac{\partial^2 \varphi}{\partial \eta_1^2} + \varepsilon^2 k_1^2 \frac{\partial^2 \varphi}{\partial \eta_2^2} = 0, \quad (3.12)$$

$$\frac{\partial^2 \psi_i}{\partial \eta_3^2} + k_2^2 \frac{\partial^2 \psi_i}{\partial \eta_1^2} + \varepsilon^2 k_2^2 \frac{\partial^2 \psi_i}{\partial \eta_2^2} = 0, \quad (i = 1, 2),$$

in the interior ($\eta_3 > 0$), along with the boundary conditions on the surface $\eta_3 = 0$

$$\frac{\partial^2 \varphi}{\partial \eta_2^2} - \frac{\partial^2 \varphi}{\partial \eta_1^2} = \frac{AP}{\varepsilon} \delta(\eta_1) \delta(\eta_2), \quad (3.13)$$

$$\frac{\partial^2 \varphi}{\partial \eta_2^2} + \frac{\partial^2 \varphi}{\partial \eta_1^2} = \frac{AP}{\varepsilon} \delta(\eta_1) \delta(\eta_2). \quad (3.14)$$

The relations between the potentials take the form

$$\frac{\partial \varphi}{\partial \eta_1} = \frac{2}{1 + k_2^2} \frac{\partial \psi_1}{\partial \eta_3}, \quad \frac{\partial \varphi}{\partial \eta_2} = \frac{2}{\varepsilon(1 + k_2^2)} \frac{\partial \psi_2}{\partial \eta_3}, \quad \eta_3 = 0. \quad (3.15)$$

The last formulae (3.12)–(3.14) support the assumption of a slow variation of all the potentials along the variable x_2 . As a result, at leading order, i.e. ignoring the terms containing the $O(\varepsilon)$ terms, equation (3.12) does not contain the derivatives with respect to η_2 .

3.2. Near-Field Steady-State Solution

As mentioned in the previous section the validity of the adapted model depends on the small physical parameter ε . Since ε is a small parameter, ε^2 will be smaller and it can be neglected in comparison to ε . Therefore we neglect $O(\varepsilon^2)$ terms in the elliptic equations for the interior given by (3.12), resulting in

$$\frac{\partial^2 \varphi}{\partial \eta_3^2} + k_1^2 \frac{\partial^2 \varphi}{\partial \eta_1^2} = 0, \quad \frac{\partial^2 \psi_i}{\partial \eta_3^2} + k_2^2 \frac{\partial^2 \psi_i}{\partial \eta_1^2} = 0, \quad (i = 1, 2). \quad (3.16)$$

Thus, the original 3D problem is reduced to two plane sub-problems in the variables (η_1, η_2) and (η_1, η_3) , respectively, over the surface and the interior.

3.2.1. Super-Rayleigh case

We will first consider the super-Rayleigh case corresponding to $c > c_R$. Since the load speed is greater than the Rayleigh wave speed the causality principle, which states that in front of the load there will not be any contribution of the potential φ , needs to be taken into account (cf. Figure 3.2). This necessitates to take the fundamental solution of the wave operator defined by (2.14) and the causality principle solution of equation (3.13) having the following form:

$$\varphi(\eta_1, \eta_2, 0) = \begin{cases} \frac{AP}{2\varepsilon} [H(\eta_2 - \eta_1) - H(\eta_2 + \eta_1)], & \eta_1 < 0 \\ 0, & \eta_1 > 0. \end{cases} \quad (3.17)$$

The solution of the potential φ evaluated on the surface $\eta_3 = 0$ can be extended into the interior of the elastic half-space through the application of Poisson's formula to the elliptic equation (3.16₁) (see equation (2.26)). On doing so, we obtain

$$\begin{aligned} \varphi(\eta_1, \eta_2, \eta_3) &= \frac{1}{\pi} \int_{-\infty}^{\infty} \frac{k_1 \eta_3}{(\xi - \eta_1)^2 + k_1^2 \eta_3^2} \varphi(\xi, \eta_2, 0) d\xi \\ &= \frac{AP}{2\pi\varepsilon} k_1 \eta_3 \int_{-\infty}^0 \frac{H(\eta_2 - \xi) - H(\eta_2 + \xi)}{(\xi - \eta_1)^2 + k_1^2 \eta_3^2} d\xi. \end{aligned} \quad (3.18)$$

In order to evaluate (3.18) it is first assumed that $\eta_2 > 0$. In this case, because of the definition of the Heaviside function, the integrand can be written as

$$H(\eta_2 - \xi) - H(\eta_2 + \xi) = \begin{cases} 1, & \xi \in (-\infty, -\eta_2) \\ 0, & \xi \in (-\eta_2, 0). \end{cases} \quad (3.19)$$

Hence the integral given by (3.18) takes the form

$$\varphi(\eta_1, \eta_2, \eta_3) = \frac{AP}{2\pi\varepsilon} k_1 \eta_3 \int_{-\infty}^{-\eta_2} \frac{1}{(\xi - \eta_1)^2 + k_1^2 \eta_3^2} d\xi. \quad (3.20)$$

Therefore the solution in the interior for $\eta_2 > 0$ is found as

$$\varphi(\eta_1, \eta_2, \eta_3) = \frac{AP}{2\pi\varepsilon} \left[\frac{\pi}{2} - \arctan \left(\frac{\eta_1 + \eta_2}{k_1\eta_3} \right) \right]. \quad (3.21)$$

In the case $\eta_2 < 0$, the integrand of equation (3.18) becomes

$$H(\eta_2 - \xi) - H(\eta_2 + \xi) = \begin{cases} 1, & \xi \in (-\infty, \eta_2) \\ 0, & \xi \in (\eta_2, 0) \end{cases} \quad (3.22)$$

and the integral now takes the form

$$\varphi(\eta_1, \eta_2, \eta_3) = \frac{AP}{2\pi\varepsilon} k_1\eta_3 \int_{-\infty}^{\eta_2} \frac{1}{(\xi - \eta_1)^2 + k_1^2\eta_3^2} d\xi. \quad (3.23)$$

Thus the solution in the interior for $\eta_2 < 0$ is obtained as

$$\varphi(\eta_1, \eta_2, \eta_3) = \frac{AP}{2\pi\varepsilon} \left[\frac{\pi}{2} - \arctan \left(\frac{\eta_1 - \eta_2}{k_1\eta_3} \right) \right]. \quad (3.24)$$

As a result, for all values of η_2 , the solution in the interior is written from equations (3.21) and (3.24) as

$$\varphi(\eta_1, \eta_2, \eta_3) = \frac{AP}{2\pi\varepsilon} \left[\frac{\pi}{2} - \arctan \left(\frac{\eta_1 + |\eta_2|}{k_1\eta_3} \right) \right]. \quad (3.25)$$

It is clearly seen from (3.25) that there will be a resonance at the Rayleigh wave speed c_R , corresponding to $\varepsilon = 0$. It is worth mentioning that in the 2D case a similar resonance is associated with a Rayleigh wave pole, see [29].

Let us now try to obtain potentials ψ_1 and ψ_2 . These potentials can be determined from the solution of the Neumann problem given by equation (3.16₂) and (3.15).

First consider the Neumann problem given by

$$\begin{aligned}
\frac{\partial^2 \psi_1}{\partial \eta_3^2} + k_2^2 \frac{\partial^2 \psi_1}{\partial \eta_1^2} &= 0, \\
\frac{\partial \psi_1}{\partial \eta_3} \Big|_{\eta_3=0} &= \frac{(1+k_2^2)}{2} \frac{\partial \varphi}{\partial \eta_1} \Big|_{\eta_3=0} \\
&= \begin{cases} -\frac{1+k_2^2}{2} \frac{AP}{2\varepsilon} [\delta(\eta_2 - \eta_1) + \delta(\eta_2 + \eta_1)], & \eta_1 < 0 \\ 0, & \eta_1 > 0 \end{cases}
\end{aligned} \tag{3.26}$$

for the potential ψ_1 . Let $\chi(\eta_1, \eta_2, \eta_3) = \partial \psi_1(\eta_1, \eta_2, \eta_3) / \partial \eta_3$. Then

$$\psi_1(\eta_1, \eta_2, \eta_3) = \int_0^{\eta_3} \chi(\eta_1, \eta_2, s) ds,$$

and the Neumann problem becomes

$$\begin{aligned}
\frac{\partial^2 \chi}{\partial \eta_3^2} + k_2^2 \frac{\partial^2 \chi}{\partial \eta_1^2} &= \frac{\partial}{\partial \eta_3} \left(\frac{\partial^2 \psi_1}{\partial \eta_3^2} + k_2^2 \frac{\partial^2 \psi_1}{\partial \eta_1^2} \right) = 0 \\
\chi(\eta_1, \eta_2, 0) &= \frac{\partial \psi_1}{\partial \eta_3} \Big|_{\eta_3=0} = \begin{cases} -\frac{AP(1+k_2^2)}{4\varepsilon} [\delta(\eta_2 - \eta_1) + \delta(\eta_2 + \eta_1)], & \eta_1 < 0 \\ 0, & \eta_1 > 0. \end{cases}
\end{aligned} \tag{3.27}$$

This is the Dirichlet problem for $\chi(\eta_1, \eta_2, \eta_3)$ and its solution is given by

$$\chi(\eta_1, \eta_2, \eta_3) = -\frac{AP(1+k_2^2)}{4\pi\varepsilon} k_2 \eta_3 \int_{-\infty}^0 \frac{\delta(\eta_2 - \xi) + \delta(\eta_2 + \xi)}{(\xi - \eta_1)^2 + k_2^2 \eta_3^2} d\xi. \tag{3.28}$$

Thus, we have

$$\begin{aligned}
\psi_1(\eta_1, \eta_2, \eta_3) &= -\frac{AP(1+k_2^2)}{4\pi\varepsilon} k_2 \int_{-\infty}^{\eta_3} s \int_{-\infty}^0 \frac{\delta(\eta_2 - \xi) + \delta(\eta_2 + \xi)}{(\xi - \eta_1)^2 + k_2^2 s^2} d\xi ds \\
&= -\frac{AP(1+k_2^2)}{4\pi\varepsilon} k_2 \int_{-\infty}^0 [\delta(\eta_2 - \xi) + \delta(\eta_2 + \xi)] \int_{-\infty}^{\eta_3} \frac{s}{(\xi - \eta_1)^2 + k_2^2 s^2} ds d\xi \\
&= -\frac{AP(1+k_2^2)}{8\pi\varepsilon k_2} \left\{ \int_{-\infty}^0 \delta(\eta_2 - \xi) \ln((\xi - \eta_1)^2 + k_2^2 \eta_3^2) d\xi + \right. \\
&\quad \left. + \int_{-\infty}^0 \delta(\eta_2 + \xi) \ln((\xi - \eta_1)^2 + k_2^2 \eta_3^2) d\xi \right\}. \quad (3.29)
\end{aligned}$$

For $\eta_2 > 0$ the first integral in (3.29) vanishes due to the definition of the Dirac-delta function. Therefore,

$$\psi_1(\eta_1, \eta_2, \eta_3) = -\frac{AP(1+k_2^2)}{8\pi\varepsilon k_2} \ln((\eta_1 + \eta_2)^2 + k_2^2 \eta_3^2), \quad \text{for } \eta_2 > 0. \quad (3.30)$$

Similarly when $\eta_2 < 0$ the second integral in equation (3.29) becomes zero. Thus,

$$\psi_1(\eta_1, \eta_2, \eta_3) = -\frac{AP(1+k_2^2)}{8\pi\varepsilon k_2} \ln((\eta_1 - \eta_2)^2 + k_2^2 \eta_3^2), \quad \text{for } \eta_2 < 0. \quad (3.31)$$

As a result of equations (3.30) and (3.31), the potential ψ_1 is obtained as

$$\psi_1(\eta_1, \eta_2, \eta_3) = -\frac{AP(1+k_2^2)}{8\pi\varepsilon k_2} \ln((\eta_1 + |\eta_2|)^2 + k_2^2 \eta_3^2). \quad (3.32)$$

Now let us consider the Neumann problem

$$\begin{aligned}
\frac{\partial^2 \psi_2}{\partial \eta_3^2} + k_2^2 \frac{\partial^2 \psi_2}{\partial \eta_1^2} &= 0, \\
\frac{\partial \psi_2}{\partial \eta_3} \Big|_{\eta_3=0} &= \frac{\varepsilon(1+k_2^2)}{2} \frac{\partial \varphi}{\partial \eta_2} \Big|_{\eta_3=0} \\
&= \begin{cases} \frac{\varepsilon(1+k_2^2)AP}{2} \frac{1}{2\varepsilon} [\delta(\eta_2 - \eta_1) - \delta(\eta_2 + \eta_1)], & \eta_1 < 0 \\ 0, & \eta_1 > 0 \end{cases} \quad (3.33)
\end{aligned}$$

for the potential ψ_2 . Let us introduce, again, an auxiliary function ω as

$$\omega(\eta_1, \eta_2, \eta_3) = \frac{\partial \psi_2(\eta_1, \eta_2, \eta_3)}{\partial \eta_3}$$

such that

$$\psi_2(\eta_1, \eta_2, \eta_3) = \int_0^{\eta_3} \omega(\eta_1, \eta_2, s) ds.$$

The Neumann problem thus reduces to the following Dirichlet problem.

$$\frac{\partial^2 \omega}{\partial \eta_3^2} + k_2^2 \frac{\partial^2 \omega}{\partial \eta_1^2} = \frac{\partial}{\partial \eta_3} \left(\frac{\partial^2 \psi_2}{\partial \eta_3^2} + k_2^2 \frac{\partial^2 \psi_2}{\partial \eta_1^2} \right) = 0, \quad (3.34)$$

$$\omega(\eta_1, \eta_2, 0) = \frac{\partial \psi_2}{\partial \eta_3} \Big|_{\eta_3=0} = \begin{cases} \frac{\varepsilon(1+k_2^2)}{2} \frac{AP}{2\varepsilon} [\delta(\eta_2 - \eta_1) - \delta(\eta_2 + \eta_1)], & \eta_1 < 0 \\ 0, & \eta_1 > 0. \end{cases} \quad (3.35)$$

The solution of the Dirichlet problem (3.34)–(3.35) is again obtained by using Poisson's formula as

$$\omega(\eta_1, \eta_2, \eta_3) = \frac{AP(1+k_2^2)}{4\pi} k_2 \eta_3 \int_{-\infty}^0 \frac{\delta(\eta_2 - \xi) - \delta(\eta_2 + \xi)}{(\xi - \eta_1)^2 + k_2^2 \eta_3^2} d\xi. \quad (3.36)$$

Thus, we have

$$\begin{aligned} \psi_2(\eta_1, \eta_2, \eta_3) &= \frac{AP(1+k_2^2)}{4\pi} k_2 \int_0^{\eta_3} s \int_{-\infty}^0 \frac{\delta(\eta_2 - \xi) - \delta(\eta_2 + \xi)}{(\xi - \eta_1)^2 + k_2^2 s^2} d\xi ds \\ &= \frac{AP(1+k_2^2)}{4\pi} k_2 \int_{-\infty}^0 [\delta(\eta_2 - \xi) - \delta(\eta_2 + \xi)] \int_0^{\eta_3} \frac{s}{(\xi - \eta_1)^2 + k_2^2 s^2} ds d\xi \\ &= \frac{AP(1+k_2^2)}{8\pi k_2} \left\{ \int_{-\infty}^0 \delta(\eta_2 - \xi) \ln((\xi - \eta_1)^2 + k_2^2 \eta_3^2) d\xi - \right. \\ &\quad \left. - \int_{-\infty}^0 \delta(\eta_2 + \xi) \ln((\xi - \eta_1)^2 + k_2^2 \eta_3^2) d\xi \right\}. \quad (3.37) \end{aligned}$$

The potential ψ_2 is readily obtained for $\eta_2 > 0$ and $\eta_2 < 0$ as

$$\psi_2(\eta_1, \eta_2, \eta_3) = -\frac{AP(1+k_2^2)}{8\pi k_2} \ln(k_2^2 \eta_3^2 + (\eta_1 + \eta_2)^2), \quad \text{for } \eta_2 > 0, \quad (3.38)$$

and

$$\psi_2(\eta_1, \eta_2, \eta_3) = \frac{AP(1+k_2^2)}{8\pi k_2} \ln(k_2^2 \eta_3^2 + (\eta_1 - \eta_2)^2), \quad \text{for } \eta_2 < 0 \quad (3.39)$$

which may be combined into a single equation

$$\psi_2(\eta_1, \eta_2, \eta_3) = -\frac{AP(1+k_2^2) \operatorname{sgn}(\eta_2)}{8\pi k_2} \ln((\eta_1 + |\eta_2|)^2 + k_2^2 \eta_3^2). \quad (3.40)$$

It is known from the Helmholtz decomposition of a vector field that a vector can be decomposed as the sum of the gradient of a scalar potential φ and the curl of a vector potential $\boldsymbol{\psi}$. The components of the displacement field, namely u_1 , u_2 and u_3 may therefore be written in terms of φ and $\boldsymbol{\psi}$ as

$$u_1 = \frac{\partial \varphi}{\partial x_1} - \frac{\partial \psi_1}{\partial x_3}, \quad u_2 = \frac{\partial \varphi}{\partial x_2} - \frac{\partial \psi_2}{\partial x_3}, \quad u_3 = \frac{\partial \varphi}{\partial x_3} + \frac{\partial \psi_1}{\partial x_2} + \frac{\partial \psi_2}{\partial x_1}. \quad (3.41)$$

In the new variables (3.11), the displacement components reduce to

$$u_1 = \frac{1}{\varepsilon} \left(\frac{\partial \varphi}{\partial \eta_1} - \frac{\partial \psi_1}{\partial \eta_3} \right), \quad u_2 = \frac{\partial \varphi}{\partial \eta_2} - \frac{1}{\varepsilon} \frac{\partial \psi_2}{\partial \eta_3}, \quad u_3 = \frac{1}{\varepsilon} \left(\frac{\partial \varphi}{\partial \eta_3} + \frac{\partial \psi_1}{\partial \eta_1} \right) + \frac{\partial \psi_2}{\partial \eta_2}. \quad (3.42)$$

Substitution of the formulae (3.25), (3.32) and (3.40) into the expressions (3.42) results in

$$u_1 = \frac{1}{\varepsilon^2} \frac{AP\eta_3}{2\pi} \left[\frac{1+k_2^2}{2} \frac{k_2}{k_2^2\eta_3^2 + (\eta_1 + |\eta_2|)^2} - \frac{k_1}{k_1^2\eta_3^2 + (\eta_1 + |\eta_2|)^2} \right], \quad (3.43)$$

$$u_2 = \frac{1}{\varepsilon} \frac{AP\eta_3 \operatorname{sgn}(\eta_2)}{2\pi} \left[\frac{1+k_2^2}{2} \frac{k_2}{k_2^2\eta_3^2 + (\eta_1 + |\eta_2|)^2} - \frac{k_1}{k_1^2\eta_3^2 + (\eta_1 + |\eta_2|)^2} \right], \quad (3.44)$$

$$u_3 = -\frac{AP(1+k_2^2)}{4\pi k_2} \frac{\eta_1 + |\eta_2|}{k_2^2\eta_3^2 + (\eta_1 + |\eta_2|)^2} - \frac{1}{\varepsilon^2} \frac{AP}{2\pi} \left[\frac{1+k_2^2}{2k_2} \frac{\eta_1 + |\eta_2|}{k_2^2\eta_3^2 + (\eta_1 + |\eta_2|)^2} - k_1 \frac{\eta_1 + |\eta_2|}{k_1^2\eta_3^2 + (\eta_1 + |\eta_2|)^2} \right]. \quad (3.45)$$

It is easily seen from the expressions (3.43)–(3.45) that the displacement u_2 is asymptotically negligible in comparison with u_1 and u_3 since $\varepsilon \ll 1$, namely $u_2 \sim \varepsilon[u_1, u_3]$. The last formulae also indicate discontinuities along the lines $\eta_2 = \pm\eta_1$ on the surface $\eta_3 = 0$. It is worth mentioning that the discontinuities only occur behind the load, $\eta_1 < 0$, due to the causality principle. The reason is that in the super-Rayleigh case since the load speed is greater than the speed of the Rayleigh wave, no contribution comes from the potentials in front of the load, see Figure 3.2.

3.2.2. Sub-Rayleigh case

Let us now consider the sub-Rayleigh case. Similar to the consideration of super-Rayleigh case, we start by solving the boundary equation (3.14). On using the fundamental solution of Laplace operator (see (2.16)), we get from (3.14)

$$\varphi(\eta_1, \eta_2, 0) = \frac{AP}{4\pi\varepsilon} \ln(\eta_1^2 + \eta_2^2). \quad (3.46)$$

The solution in the interior is expressed via the Poisson formula, taking the form

$$\begin{aligned} \varphi(\eta_1, \eta_2, \eta_3) &= \frac{1}{\pi} \int_{-\infty}^{\infty} \frac{k_1\eta_3}{(\xi - \eta_1)^2 + k_1^2\eta_3^2} \varphi(\xi, \eta_2, 0) d\xi \\ &= \frac{AP}{4\pi^2\varepsilon} k_1\eta_3 \int_{-\infty}^{\infty} \frac{\ln(\xi^2 + \eta_2^2)}{(\xi - \eta_1)^2 + k_1^2\eta_3^2} d\xi. \end{aligned} \quad (3.47)$$

In order to evaluate the integral (3.47) we will employ the residue calculus. To this end let us define a complex valued function $f(z)$ as

$$f(z) = \frac{\ln(z + i\eta_2)}{(z - \eta_1)^2 + k_1^2\eta_3^2},$$

and consider the following integral

$$\int_C f(z)dz,$$

where C is a contour in the complex plane whose choice will depend on the location of the branch cut of the function $f(z)$. The function $f(z)$ has a branch point at $z = -i\eta_2$ and therefore the value of the integral will depend on the sign of η_2 .

First consider $\eta_2 > 0$. In this case C must be a closed contour consisting of the interval $[-R, R]$ and the semicircle in the upper half plane, C_R , so that the integral converges, see Figure 3.3. The branch point $z = -i\eta_2$ of $f(z)$, in this case, is on the negative imaginary axis and also $f(z)$ has two poles at $z_1 = \eta_1 + k_1\eta_3$ and $z_2 = \eta_1 - k_1\eta_3$. The branch cut does not lie in the region bounded by the contour C and only the pole z_1 is inside the region bounded by the contour C . The integral may then be computed using the residue theorem:

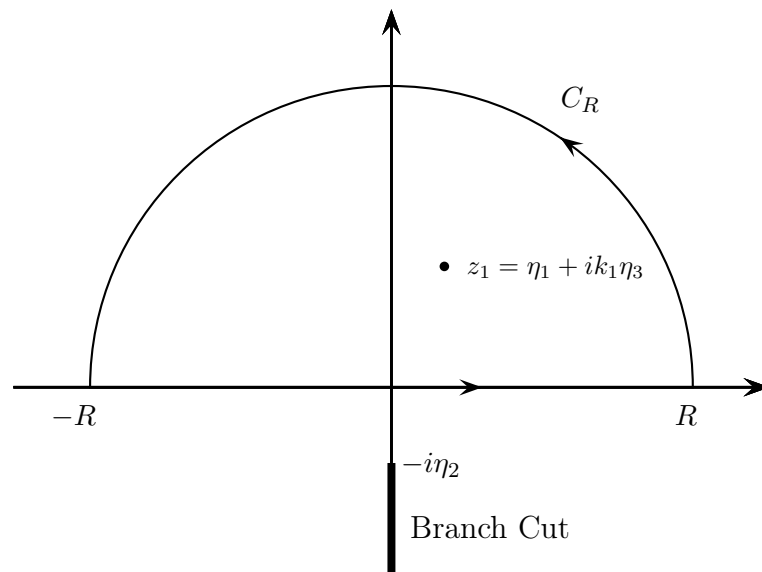


Figure 3.3. Semicircular contour C for $\eta_2 > 0$.

$$\int_C f(z)dz = \int_{-R}^R f(\xi)d\xi + \int_{C_R} f(z)dz = 2\pi i \operatorname{res}(f(z), z_1). \quad (3.48)$$

The residue of $f(z)$ at the pole z_1 is

$$\operatorname{res}(f(z), z_1) = \lim_{z \rightarrow z_1} (z - z_1)f(z) = \frac{1}{2ik_1\eta_3} \ln(\eta_1 + i(k_1\eta_3 + \eta_2)),$$

and the integral over C_R is zero as $R \rightarrow \infty$ since

$$\left| \int_{C_R} f(z)dz \right| \leq \int_{C_R} |f(z)|dz \leq \pi R \frac{\ln R}{R^2 - k_1^2\eta_3^2} \rightarrow 0, \quad \text{as } R \rightarrow \infty.$$

As a result we obtain from equation (3.48)

$$\int_{-\infty}^{\infty} \frac{\ln(\xi + i\eta_2)}{(\xi - \eta_1)^2 + k_1^2\eta_3^2} d\xi = \frac{\pi}{k_1\eta_3} \ln(\eta_1 + i(k_1\eta_3 + \eta_2)), \quad (3.49)$$

from which we deduce that

$$\int_{-\infty}^{\infty} \frac{1/2 \ln(\xi^2 + \eta_2^2) + i \arg(\xi + i\eta_2)}{(\xi - \eta_1)^2 + k_1^2\eta_3^2} d\xi = \frac{\pi}{k_1\eta_3} \left[\frac{1}{2} \ln(\eta_1^2 + (k_1\eta_3 + \eta_2)^2) + i \arg(\eta_1 + i(k_1\eta_3 + \eta_2)) \right]. \quad (3.50)$$

Finally the sought for integral is found as

$$\int_{-\infty}^{\infty} \frac{\ln(\xi^2 + \eta_2^2)}{(\xi - \eta_1)^2 + k_1^2\eta_3^2} d\xi = \frac{\pi}{k_1\eta_3} \ln(\eta_1^2 + (k_1\eta_3 + \eta_2)^2). \quad (3.51)$$

Going back to equation (3.47) we may now write the potential φ in the interior for $\eta_2 > 0$ as

$$\varphi(\eta_1, \eta_2, \eta_3,) = \frac{AP}{4\pi\epsilon} \ln(\eta_1^2 + (k_1\eta_3 + \eta_2)^2). \quad (3.52)$$

Now consider $\eta_2 < 0$. In this case, in order to make the integral convergent we choose a closed contour C' consisting of the interval $[-R, R]$ and the semicircle in the lower half plane, C_R , see Figure 3.4. Hence the branch cut is outside the closed contour C' and only the pole z_2 is in the region bounded by the closed contour C' .

Employing once again the residue theorem we write

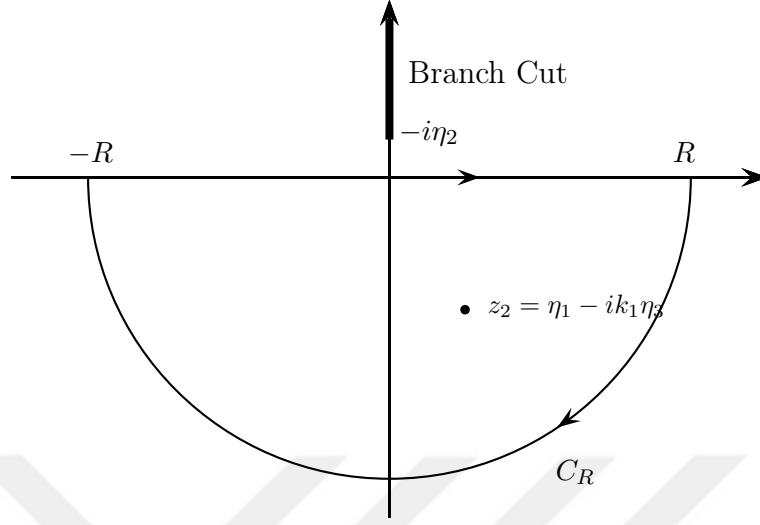


Figure 3.4. Semicircular contour C' for $\eta_2 < 0$.

$$\int_C f(z)dz = \int_{-R}^R f(\xi)d\xi + \int_{-C_R} f(z)dz = -2\pi i \operatorname{res}(f(z), z_2). \quad (3.53)$$

The residue of $f(z)$ at z_2 is easily evaluated as

$$\operatorname{res}(f(z), z_2) = \lim_{z \rightarrow z_2} f(z) = -\frac{1}{2ik_1\eta_3} \ln(\eta_1 - i(k_1\eta_3 - \eta_2)).$$

We conclude from equation (3.53), as $R \rightarrow \infty$, that

$$\int_{-\infty}^{\infty} \frac{\ln(\xi + i\eta_2)}{(\xi - \eta_1)^2 + k_1^2\eta_3^2} d\xi = \frac{\pi}{k_1\eta_3} \ln(\eta_1 - i(k_1\eta_3 - \eta_2)). \quad (3.54)$$

Hence

$$\int_{-\infty}^{\infty} \frac{\ln(\xi^2 + \eta_2^2)}{(\xi - \eta_1)^2 + k_1^2\eta_3^2} d\xi = \frac{\pi}{k_1\eta_3} \ln(\eta_1^2 + (k_1\eta_3 - \eta_2)^2). \quad (3.55)$$

The solution φ in the interior for $\eta_2 < 0$ may, therefore, be written as

$$\varphi(\eta_1, \eta_2, \eta_3) = \frac{AP}{4\pi\varepsilon} \ln(\eta_1^2 + (k_1\eta_3 - \eta_2)^2). \quad (3.56)$$

Consequently the solution of φ for all η_2 now follows from equations (3.52) and (3.56) given by

$$\varphi(\eta_1, \eta_2, \eta_3) = \frac{AP}{4\pi\varepsilon} \ln(\eta_1^2 + (k_1\eta_3 + |\eta_2|)^2). \quad (3.57)$$

We should now check whether the solution φ is continuous at $\eta_2 = 0$. Taking $\eta_2 = 0$ in the integral given by equation (3.47) we get

$$\begin{aligned} \int_{-\infty}^{\infty} \frac{\ln(\xi^2)}{(\xi - \eta_1)^2 + k_1^2\eta_3^2} d\xi &= \int_{-\infty}^0 \frac{\ln(\xi^2)}{(\xi - \eta_1)^2 + k_1^2\eta_3^2} d\xi + \int_0^{\infty} \frac{\ln(\xi^2)}{(\xi - \eta_1)^2 + k_1^2\eta_3^2} d\xi \\ &= \int_0^{\infty} \frac{\ln(\xi^2)}{(\xi + \eta_1)^2 + k_1^2\eta_3^2} d\xi + \int_0^{\infty} \frac{\ln(\xi^2)}{(\xi - \eta_1)^2 + k_1^2\eta_3^2} d\xi \end{aligned} \quad (3.58)$$

which can again be evaluated with the help of the residue calculus.

Let us consider the first integral on the right hand side of in equation (3.58) and define a complex valued function $g(z)$ as

$$g(z) = \frac{\ln^2(z)}{(z + \eta_1)^2 + k_1^2\eta_3^2}$$

which has a branch point at $z = 0$, and the simple poles at $z_1 = -\eta_1 + ik_1\eta_3$ and $z_2 = -\eta_1 - ik_1\eta_3$. The branch cut of $g(z)$ is chosen as the positive real axis, therefore we consider the contour $C_{r,R}$ consisting of the circle C_r , $|z| = r$, and C_R , $|z| = R$, and the segments L_1 and L_2 respectively, see Figure 3.5. Since R is so large and r is so small that two poles of $g(z)$ lie inside $C_{r,R}$.

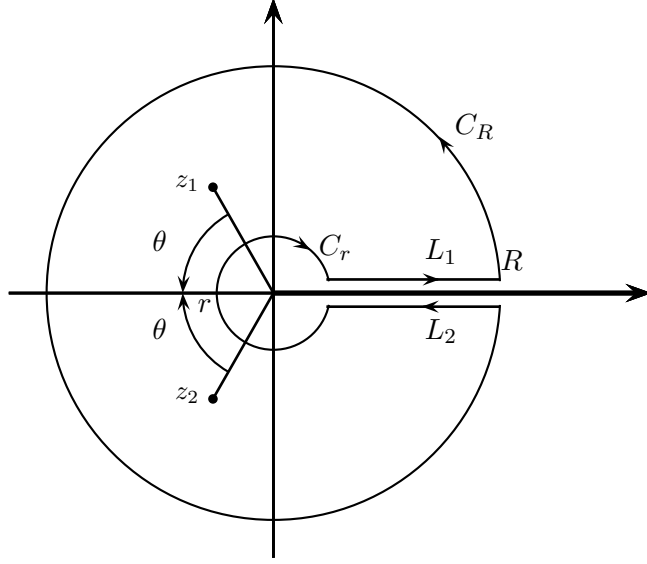


Figure 3.5. Keyhole contour with the poles $-\eta_1 + ik_1\eta_3$ and $-\eta_1 - ik_1\eta_3$.

By the residue theorem

$$\int_{C_{r,R}} g(z)dz = \int_{L_1} g(\xi)d\xi + \int_{C_R} g(z)dz + \int_{L_2} g(\xi)d\xi + \int_{C_r} g(z)dz = 2\pi i \sum_{k=1}^2 \text{res}(g(z), z_k). \quad (3.59)$$

The integrals along C_r and C_R tend to zero as $r \rightarrow 0$ and $R \rightarrow \infty$ since $r \max_{z \in C_r} |g(z)| \rightarrow 0$ as $r \rightarrow 0$ and $R \max_{z \in C_R} |g(z)| \rightarrow 0$ as $R \rightarrow \infty$ (see [30]). On the upper line, L_1 , the argument of $z = x + i0$ is zero and on the lower line, L_2 , the argument of $z = x - i0$ is 2π . Thus

$$\begin{aligned} \text{On } L_1 : \ln^2(z) &= (\ln(x + i0) + i \arg(x + i0))^2 = (\ln(x))^2, \\ &= \ln^2(x) \end{aligned}$$

and

$$\begin{aligned} \text{On } L_2 : \ln^2(z) &= (\ln(x - i0) + i \arg(x - i0))^2 = (\ln(x) + i2\pi)^2, \\ &= \ln^2(x) + 4i\pi \ln(x) - 4\pi^2 \end{aligned}$$

The residue of $g(z)$ at the poles z_1 and z_2 are

$$\text{res}(g(z), z_1) = \frac{\ln^2(z_1)}{2(z_1 + \eta_1)} = \frac{\ln^2(z_1)}{2ik_1\eta_3} = \frac{1}{2ik_1\eta_3} [\ln(\rho) + i(\pi - \theta)]^2,$$

and

$$\operatorname{res}(g(z), z_2) = \frac{\ln^2(z_2)}{2(z_2 + \eta_1)} = \frac{\ln^2(z_1)}{-2ik_1\eta_3} = -\frac{1}{2ik_1\eta_3} [\ln(\rho) + i(\pi + \theta)]^2,$$

where $\rho = \sqrt{\eta_1^2 + k_1^2\eta_3^2}$ and $\theta = \arctan(\eta_1/k_1\eta_3)$. Consequently we obtain from equation (3.59)

$$\begin{aligned} \int_{C_{r,R}} g(z) dz &= \int_r^R \frac{\ln^2(\xi)}{(\xi + \eta_1)^2 + k_1^2\eta_3^2} d\xi + \int_R^r \frac{\ln^2(\xi) + 4i\pi \ln(\xi) - 4\pi^2}{(\xi + \eta_1)^2 + k_1^2\eta_3^2} d\xi \\ &= \frac{2\pi i}{2ik_1\eta_3} \{ [\ln(\rho) + i(\pi - \theta)]^2 - [\ln(\rho) + i(\pi + \theta)]^2 \}. \end{aligned}$$

If we go over to the limit as $r \rightarrow 0$ and $R \rightarrow \infty$, we obtain

$$\begin{aligned} \int_0^\infty \frac{\ln^2(\xi)}{(\xi + \eta_1)^2 + k_1^2\eta_3^2} d\xi - \int_0^\infty \frac{\ln^2(\xi) + 4i\pi \ln(\xi) - 4\pi^2}{(\xi + \eta_1)^2 + k_1^2\eta_3^2} d\xi &= \frac{\pi}{k_1\eta_3} 4\theta (\pi - i \ln(\rho)) \\ - 4i\pi \int_0^\infty \frac{\ln(\xi)}{(\xi + \eta_1)^2 + k_1^2\eta_3^2} d\xi + 4\pi^2 \int_0^\infty \frac{1}{(\xi + \eta_1)^2 + k_1^2\eta_3^2} d\xi &= -\frac{4i\pi\theta \ln(\rho)}{k_1\eta_3} + \frac{4\pi^2\theta}{k_1\eta_3}, \end{aligned}$$

from which we deduce that

$$\int_0^\infty \frac{\ln(\xi)}{(\xi + \eta_1)^2 + k_1^2\eta_3^2} d\xi = \frac{\theta}{k_1\eta_3} \ln(\rho). \quad (3.60)$$

Let us now consider the second integral in equation (3.58) and again define a complex valued function $h(z)$ as

$$h(z) = \frac{\ln^2(z)}{(z - \eta_1)^2 + k_1^2\eta_3^2}.$$

Since the branch cut of the logarithmic function again lies on the positive real axis we consider the same closed contour $C_{r,R}$ as in the previous integral. In this case the poles of the function $h(z)$, which are $z_3 = \eta_1 + ik_1\eta_3$ and $z_4 = \eta_1 - ik_1\eta_3$, are different from the poles of the function $g(z)$ but it does not have a great affect in the calculation of the integral since there will be only changes in the argument of

the poles (see Figure 3.6). Employing the residue theorem, integral over the $C_{r,R}$ is written as

$$\begin{aligned} \int_{C_{r,R}} h(z)dz &= \int_{L_1} h(\xi)d\xi + \int_{C_R} h(z)dz + \\ &+ \int_{L_2} h(\xi)d\xi + \int_{C_r} h(z)dz = 2\pi i \sum_{k=3}^4 \text{res}(h(z), z_k). \end{aligned} \quad (3.61)$$

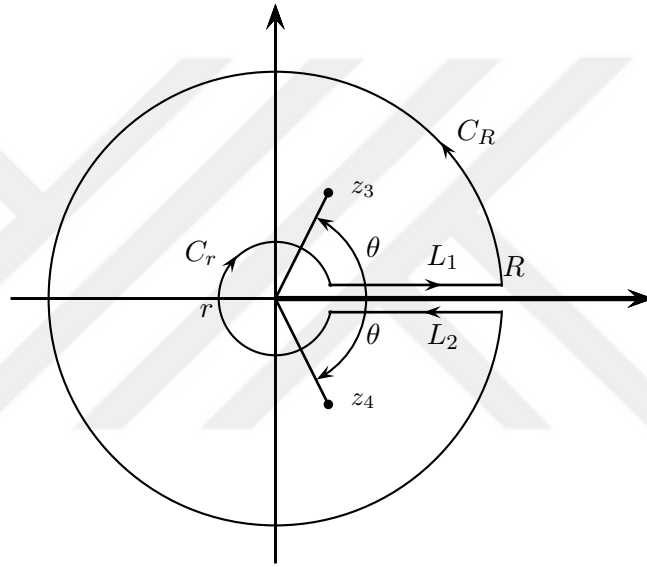


Figure 3.6. Keyhole contour with the poles $\eta_1 + ik_1\eta_3$ and $\eta_1 - ik_1\eta_3$.

The integrals along C_r and C_R again tend to zero as $r \rightarrow 0$ and $R \rightarrow \infty$ similar to the previous calculation of the first integral in (3.58). At the same time on the upper line, L_1 , since the argument of $z = x + i0$ is zero $\ln^2(z) = (\ln(x))^2$ and on the lower line, L_2 , since the argument of $z = x - i0$ is 2π $\ln^2(z) = \ln^2(x) + 4i\pi \ln(x) - 4\pi^2$. The residue of $h(z)$ at the poles z_3 and z_4 are

$$\text{res}(h(z), z_3) = \frac{\ln^2(z_3)}{2(z_3 - \eta_1)} = \frac{\ln^2(z_3)}{2ik_1\eta_3} = \frac{1}{2ik_1\eta_3} [\ln(\rho) + i\theta]^2,$$

and

$$\text{res}(h(z), z_4) = \frac{\ln^2(z_4)}{2(z_4 - \eta_1)} = \frac{\ln^2(z_4)}{-2ik_1\eta_3} = -\frac{1}{2ik_1\eta_3} [\ln(\rho) + i(2\pi - \theta)]^2,$$

where $\rho = \sqrt{\eta_1^2 + k_1^2 \eta_3^2}$ and $\theta = \arctan(\eta_1/k_1 \eta_3)$. As a result we get from equation (3.61)

$$\begin{aligned} \int_{C_{r,R}} h(z) dz &= \int_r^R \frac{\ln^2(\xi)}{(\xi - \eta_1)^2 + k_1^2 \eta_3^2} d\xi + \int_R^r \frac{\ln^2(\xi) + 4i\pi \ln(x) - 4\pi^2}{(\xi - \eta_1)^2 + k_1^2 \eta_3^2} d\xi \\ &= \frac{2\pi i}{2ik_1 \eta_3} \{ [\ln(\rho) + i\theta]^2 - [\ln(\rho) + i(2\pi - \theta)]^2 \}. \end{aligned}$$

Taking into account the limit as $r \rightarrow 0$ and $R \rightarrow \infty$, we obtain

$$\begin{aligned} \int_0^\infty \frac{\ln^2(\xi)}{(\xi - \eta_1)^2 + k_1^2 \eta_3^2} d\xi - \int_0^\infty \frac{\ln^2(\xi) + 4i\pi \ln(\xi) - 4\pi^2}{(\xi - \eta_1)^2 + k_1^2 \eta_3^2} d\xi &= \frac{\pi}{k_1 \eta_3} 4(\theta - \pi) (-\pi + i \ln(\rho)), \\ -4i\pi \int_0^\infty \frac{\ln(\xi)}{(\xi - \eta_1)^2 + k_1^2 \eta_3^2} d\xi + 4\pi^2 \int_0^\infty \frac{1}{(\xi - \eta_1)^2 + k_1^2 \eta_3^2} d\xi &= \frac{\pi}{k_1 \eta_3} 4(\theta - \pi) (-\pi + i \ln(\rho)), \end{aligned}$$

which gives

$$\int_0^\infty \frac{\ln(\xi)}{(\xi + \eta_1)^2 - k_1^2 \eta_3^2} d\xi = \frac{\pi - \theta}{k_1 \eta_3} \ln(\rho). \quad (3.62)$$

Combining equations (3.47), (3.58), (3.60) and (3.62), the potential φ at $\eta_2 = 0$ is obtained as

$$\begin{aligned} \varphi(\eta_1, 0, \eta_3) &= \frac{AP}{4\pi^2 \varepsilon} k_1 \eta_3 \left[\frac{\theta}{k_1 \eta_3} \ln(\rho) + \frac{\pi - \theta}{k_1 \eta_3} \ln(\rho) \right] \\ &= \frac{AP}{4\pi \varepsilon} \ln(\eta_1^2 + k_1^2 \eta_3^2). \end{aligned} \quad (3.63)$$

These results show that the obtained solution for the interior is continuous everywhere but is not differentiable in η_2 along the plane $\eta_2 = 0$ which is a result of neglecting $O(\varepsilon^2)$ terms in equation (3.12₁).

The potentials ψ_1 and ψ_2 , similar to the super-Rayleigh case, may be determined from the solution of the Neumann problem (3.16) and (3.15). However here we only present the expressions of the potentials without dwelling into the lengthy but the straightforward calculations. Therefore ψ_1 and ψ_2 for the sub-Rayleigh case are

given by

$$\psi_1(\eta_1, \eta_2, \eta_3) = \frac{AP(1+k_2^2)}{4\pi\epsilon k_2} \arctan\left(\frac{k_2\eta_3 + |\eta_2|}{\eta_1}\right), \quad (3.64)$$

and

$$\psi_2(\eta_1, \eta_2, \eta_3) = \frac{AP(1+k_2^2) \operatorname{sgn}(\eta_2)}{8\pi k_2} \ln(\eta_1^2 + (k_2\eta_3 + |\eta_2|)^2). \quad (3.65)$$

respectively. Thus all potentials for the sub-Rayleigh case are determined and the displacements can be written from equation (3.42) as

$$u_1 = \frac{1}{\epsilon^2} \frac{AP}{2\pi} \left[\frac{\eta_1}{\eta_1^2 + (k_1\eta_3 + |\eta_2|)^2} - \frac{1+k_2^2}{2} \frac{\eta_1}{\eta_1^2 + (k_2\eta_3 + |\eta_2|)^2} \right], \quad (3.66)$$

$$u_2 = \frac{1}{\epsilon} \frac{AP \operatorname{sgn}(\eta_2)}{2\pi} \left[\frac{k_1\eta_3 + |\eta_2|}{\eta_1^2 + (k_1\eta_3 + |\eta_2|)^2} - \frac{1+k_2^2}{2} \frac{k_2\eta_3 + |\eta_2|}{\eta_1^2 + (k_2\eta_3 + |\eta_2|)^2} \right], \quad (3.67)$$

$$u_3 = -\frac{AP(1+k_2^2)}{4\pi k_2} \frac{k_2\eta_3 + |\eta_2|}{\eta_1^2 + (k_2\eta_3 + |\eta_2|)^2} + \frac{1}{\epsilon^2} \frac{AP}{2\pi} \left[k_1 \frac{k_1\eta_3 + |\eta_2|}{\eta_1^2 + (k_1\eta_3 + |\eta_2|)^2} - \frac{1+k_2^2}{2k_2} \frac{k_2\eta_3 + |\eta_2|}{\eta_1^2 + (k_2\eta_3 + |\eta_2|)^2} \right]. \quad (3.68)$$

It can be seen from the last expressions that the asymptotically secondary displacement u_2 has a discontinuity at $\eta_2 = 0$ because of the presence of $\operatorname{sgn}(\eta_2)$ in (3.67). This originates from the aforementioned discontinuity of the derivative $\partial\varphi/\partial\eta_2$ (cf. expressions for displacements (3.42)).

3.3. Investigation of the Accuracy of the Asymptotic Solutions

In the previous section, the original 3D problem was reduced to two plane problems by neglecting $O(\epsilon^2)$ terms in the elliptic equations for the interior. Then the approximate solutions were presented for the plane sub-problems by solving 2D Dirichlet problems. We will now investigate the accuracy of the approximate solutions obtained by neglecting $O(\epsilon^2)$ terms. To this end we will compare the solution of the 3D the boundary value problem, keeping $O(\epsilon^2)$ terms, with the approximate solution (3.57). We will carry out the investigation only for the sub-Rayleigh case. A similar procedure may be applied straightforwardly to the super-Rayleigh case.

If $O(\epsilon^2)$ is not neglected in equation (3.12₁), we have a 3D boundary value prob-

lem (3.12)₁, (3.14) we reproduce here

$$\begin{aligned}\frac{\partial^2 \varphi}{\partial \eta_3^2} + k_1^2 \frac{\partial^2 \varphi}{\partial \eta_1^2} + \varepsilon^2 k_1^2 \frac{\partial^2 \varphi}{\partial \eta_2^2} &= 0, \\ \frac{\partial^2 \varphi}{\partial \eta_2^2} + \frac{\partial^2 \varphi}{\partial \eta_1^2} &= \frac{AP}{\varepsilon} \delta(\eta_1) \delta(\eta_2).\end{aligned}\tag{3.69}$$

On introducing scaled variables

$$\eta_1 = k_1 \sigma, \quad \eta_2 = \varepsilon k_1 \nu$$

equations (3.69) are written as

$$\begin{aligned}\frac{\partial^2 \varphi}{\partial \eta_3^2} + \frac{\partial^2 \varphi}{\partial \sigma^2} + \frac{\partial^2 \varphi}{\partial \nu^2} &= 0, \\ \frac{\partial^2 \varphi}{\partial \nu^2} + \varepsilon^2 \frac{\partial^2 \varphi}{\partial \sigma^2} &= AP \delta(\sigma) \delta(\nu).\end{aligned}\tag{3.70}$$

In order to reduce (3.70₂) to a standard elliptic equation, we again make a change of variable as $\sigma = \varepsilon \gamma$. Thus equation (3.70₂) takes the form

$$\frac{\partial^2 \varphi}{\partial \nu^2} + \frac{\partial^2 \varphi}{\partial \gamma^2} = \frac{AP}{\varepsilon} \delta(\gamma) \delta(\nu),\tag{3.71}$$

whose solution is given by means of the fundamental solution of the Laplace operator as

$$\varphi(\gamma, \nu, \eta_3) = \frac{AP}{4\pi\varepsilon} \ln(\gamma^2 + \nu^2).\tag{3.72}$$

Therefore in variables (σ, ν) the boundary solution becomes

$$\varphi(\sigma, \nu, \eta_3) = \frac{AP}{4\pi\varepsilon} \ln\left(\frac{\sigma^2}{\varepsilon^2} + \nu^2\right).\tag{3.73}$$

Hence, the solution of the Rayleigh wave field over the interior can be written with the help of the boundary solution (3.73) and Poisson's formula as

$$\begin{aligned}\varphi(\eta_1, \eta_2, \eta_3) &= \frac{1}{2\pi} \int_{-\infty}^{\infty} \int_{-\infty}^{\infty} \frac{\eta_3 \varphi(\xi_1, \xi_2, 0)}{[(\xi_1 - \sigma)^2 + (\xi_2 - \nu)^2 + \eta_3^2]^{\frac{3}{2}}} d\xi_1 d\xi_2 \\ &= \frac{AP\eta_3}{8\pi^2\varepsilon} \int_{-\infty}^{\infty} \int_{-\infty}^{\infty} \frac{\log(\xi_1^2/\varepsilon^2 + \xi_2^2)}{\left[\left(\xi_1 - \frac{\eta_1}{k_1}\right)^2 + \left(\xi_2 - \frac{\eta_2}{\varepsilon k_1}\right)^2 + \eta_3^2\right]^{\frac{3}{2}}} d\xi_1 d\xi_2.\end{aligned}\quad (3.74)$$

Let us now compare the approximation (3.57) and the solution of the 3D boundary value problem (3.74). Since the components of the displacement can be expressed in terms of the one wave potentials since the wave potentials are related each other with a relation given in (3.15) we only consider the derivative of (3.74). Hence numerical values of derivative $\chi = \frac{4\pi\varepsilon}{AP} \frac{\partial\varphi}{\partial\eta_2}$ are shown in Figure 3.7.

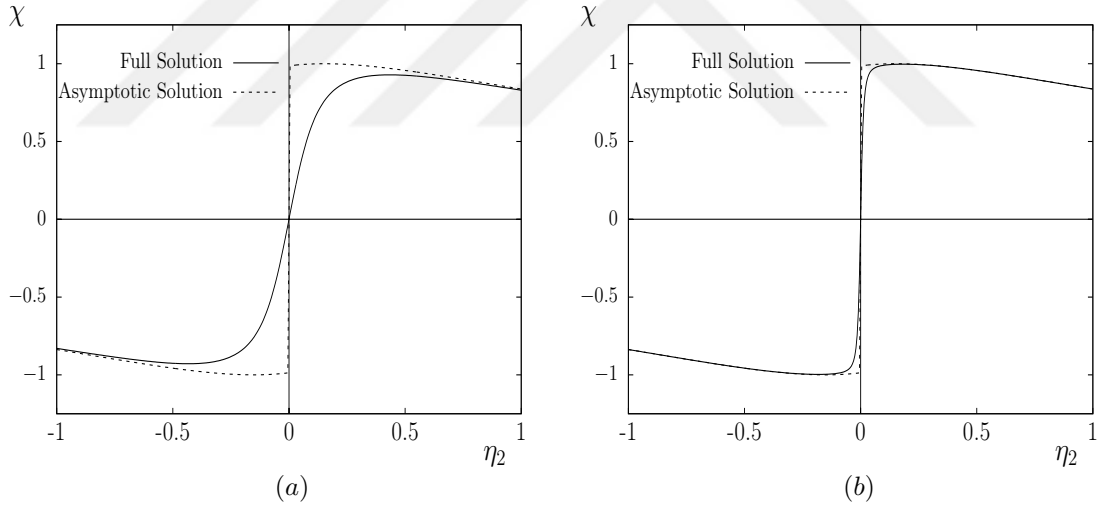


Figure 3.7. Comparison of the derivatives of full and asymptotic solutions (3.57) and (3.74) in the sub-Rayleigh case, for $\nu = 0.25$, $\eta_1 = \eta_3 = 1$ and (a) $\varepsilon = 0.1$, (b) $\varepsilon = 0.01$.

It may clearly be seen from Figure 3.7 that for $\varepsilon \ll 1$ the full solution corresponding to the derivative of (3.74) just smoothes the jump at $\eta_2 = 0$ arising when differentiating (3.74) with respect to η_2 . It can also be seen that when the load speed is closer the Rayleigh wave speed, corresponding to smaller values of ε , the approximate solution becomes more accurate.

3.4. Transient Surface Motion

In Section 2.2 solutions of the considered problem were investigated when the speed of the load is close the Rayleigh wave speed, corresponding to $\varepsilon \ll 1$. Thus in the near-field the steady-state solutions were obtained for the sub and super-Rayleigh cases respectively. As can be seen from the obtained solutions, (3.43)–(3.45) and (3.66)–(3.68), there would be a resonance at $\varepsilon = 0$, corresponding to the Rayleigh wave speed being equal to load speed, i.e. $c_R = c$. This resonance for $c = c_R$ motivates a transient analysis of the 3D moving load problem. Therefore in this section we focus on finding the solution of surface equation (3.5). The fundamental solution of the 2D wave equation is written from equation (2.12) as

$$\mathcal{F}(x_1, x_2, t) = -\frac{c_R H\left(c_R t - \sqrt{x_1^2 + x_2^2}\right)}{2\pi \sqrt{c_R^2 t^2 - x_1^2 - x_2^2}}. \quad (3.75)$$

Then the solution of equation (3.5) may be expressed as a convolution, i.e.

$$\begin{aligned} \varphi(x_1, x_2, 0, t) &= \int_0^t \mathcal{F}(x_1 - ct, x_2, t - \tau) d\tau \\ &= -\frac{APc_R}{2\pi} \int_0^t \frac{H\left(c_R(t - \tau) - \sqrt{(x_1 - c\tau)^2 + x_2^2}\right)}{\sqrt{c_R^2(t - \tau)^2 - (x_1 - c\tau)^2 - x_2^2}} d\tau, \end{aligned} \quad (3.76)$$

or equivalently,

$$\varphi(\lambda, x_2, 0, t) = -\frac{APc_R}{2\pi} \int_0^t \frac{H(c_R s - \sqrt{(\lambda + cs)^2 + x_2^2})}{\sqrt{(c_R^2 - c^2)s^2 - 2sc\lambda - \lambda^2 - x_2^2}} ds, \quad (3.77)$$

where $\lambda = x_1 - ct$ and $s = t - \tau$.

First consider the resonant regime $c = c_R$. In this case argument of the square root function may be positive when $\lambda < 0$ and similarly the argument of the Heaviside function is positive when $t \geq -\frac{\lambda^2 + x_2^2}{2c_R\lambda}$. Under these assumptions the integral

in (3.77) takes the following form

$$\varphi(\lambda, x_2, 0, t) = -\frac{APc_R}{2\pi} \int_{-\frac{\lambda^2+x_2^2}{2c_R\lambda}}^t \frac{1}{\sqrt{-2sc_R\lambda - \lambda^2 - x_2^2}} ds, \quad (3.78)$$

from which we deduce that

$$\varphi(\lambda, x_2, 0, t) = \frac{AP}{2\pi\lambda} \sqrt{-\lambda^2 - 2c_R t \lambda - x_2^2}. \quad (3.79)$$

Taking the limit as $t \rightarrow \infty$ we get

$$\varphi(\lambda, x_2, 0, t) \sim C\sqrt{t}, \quad C = \frac{AP}{\pi} \sqrt{-\frac{c_R}{2\lambda}}. \quad (3.80)$$

Thus, there is no steady-state limit as $t \rightarrow \infty$ for a load moving with the Rayleigh wave speed. In this case the solution grows in time as \sqrt{t} whereas the solution of the related plane strain problem demonstrates a linear growth in time, see [15].

In the sub-Rayleigh case the argument of the Heaviside function is positive i.e., that the Heaviside function is different from zero when

$$s > p + \sqrt{p^2 + r} \quad \text{and} \quad s < p - \sqrt{p^2 + r}, \quad (3.81)$$

where

$$p = \frac{\lambda c}{c_R^2 - c^2} \quad \text{and} \quad r = \frac{\lambda^2 + x_2^2}{c_R^2 - c^2}. \quad (3.82)$$

Since $\lambda < 0$, s will be positive only for the first inequality. Thus we have

$$\begin{aligned} \varphi(\lambda, x_2, 0, t) &= -\frac{APc_R}{2\pi} \int_{p+\sqrt{p^2+r}}^t \frac{1}{\sqrt{(c_R^2 - c^2)s^2 - 2sc\lambda - \lambda^2 - x_2^2}} ds \\ &= \frac{AP}{2\pi\varepsilon} \ln \frac{\sqrt{\lambda^2 c^2 + (c_R^2 - c^2)(\lambda^2 + x_2^2)}}{(c_R^2 - c^2)t - \lambda c + \sqrt{c_R^2 - c^2} \sqrt{(c_R^2 - c^2)t^2 - 2\lambda ct - \lambda^2 - x_2^2}}, \end{aligned} \quad (3.83)$$

where

$$t \geq \frac{\lambda c + \sqrt{\lambda^2 c^2 + (c_R^2 - c^2)(\lambda^2 + x_2^2)}}{c_R^2 - c^2}. \quad (3.84)$$

It follows from (3.83) that as $t \rightarrow \infty$

$$\varphi(\lambda, x_2, 0) \sim \frac{AP}{2\pi\varepsilon} \left[\ln \sqrt{\frac{\lambda^2}{\varepsilon^2} + x_2^2} - \ln \left(2\sqrt{c_R^2 - c^2 t} \right) \right]. \quad (3.85)$$

As might be expected, the first term in R. H. S. of (3.85) coincides with the steady-state solution (3.46). The extra time-dependent logarithmic term is homogenous over the surface and as a consequence, does not affect the displacement. A similar procedure may be applied to the integral (3.77) in the super-Rayleigh case and it is expect that the integral (3.77) takes the value (3.17) at steady-state limit.

3.5. Numerical Results of the Uncoated Half-Space

In this section numerical values of the steady state solution (3.43)-(3.45) and (3.66)-(3.68) are illustrated. The frequency equation of surface waves is expressed by

$$\frac{c_R^2}{c_2^2} \left\{ \left(\frac{c_R}{c_2} \right)^6 - 8 \left(\frac{c_R}{c_2} \right)^4 + (24 - 16k^{-2}) \left(\frac{c_R}{c_2} \right)^2 - 16(1 - k^{-2}) \right\} = 0, \quad (3.86)$$

where $k^2 = 2(1-\nu)/(1-2\nu)$, see [25]. Equation (3.86) is reduced to a cubic equation in $(c_R/c_2)^2$ the roots of which may be real or complex and depend on the Poisson ratio ν . However any complex values of $(c_R/c_2)^2$ will not acceptable in the general theory of vibrations of stable systems and also $(c_R/c_2)^2$ must be less than 1, see [2]. If we set $\nu = 0.25$ the suitable root of equation (3.86) will be $2 - 2/\sqrt{3}$ corresponding to $c_R = 0.9194c_2$.

The principal displacements displayed in the figures to follow are normalized as

$$U_i(\eta_1, \eta_2, \eta_3) = \frac{2\pi}{AP} u_i(\eta_1, \eta_2, \eta_3), \quad i = 1, 3$$

Let us first consider the super-Rayleigh case. In this case, since $c > c_R$ and $c_R = 0.9194c_2$, we set the speed of the load $c = 0.924c_2$, and therefore $\varepsilon = 0.1$.

Figure (3.8) shows the variation of the vertical displacement U_3 along the trajectory of the load depending on depth. As expected, it is observed that there is a decay away from the surface, which is a characteristic of the Rayleigh wave field.

In other words, Figure 3.8 shows that the effect of the surface wave disappears as the depth increases along the x_3 -axis. A singular behaviour under a point force ($\eta_k = 0, k = 1, 2, 3$) is clearly seen in Figure 3.8 *a*. Figure 3.8 *b* indicates surface discontinuity at $\eta_1 = -\eta_2 = -1, \eta_3 = 0$. Because of the causality principle the effect of the Rayleigh wave field only occurs in the contour of the Mach cone behind of the load $\eta_1 < 0$ (cf. Figure 3.2). Therefore in Figure 3.8 *b* there is no disturbance in front of the load corresponding to $\eta_1 > 0$.

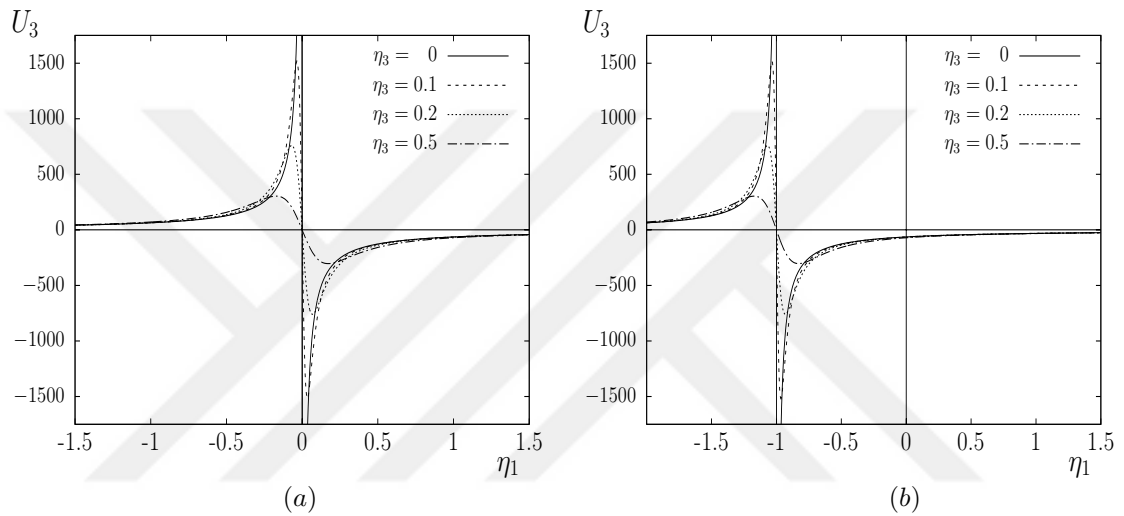


Figure 3.8. The scaled displacement U_3 vs. η_1 in the super-Rayleigh case for (a) $\eta_2 = 0$, (b) $\eta_2 = 1$.

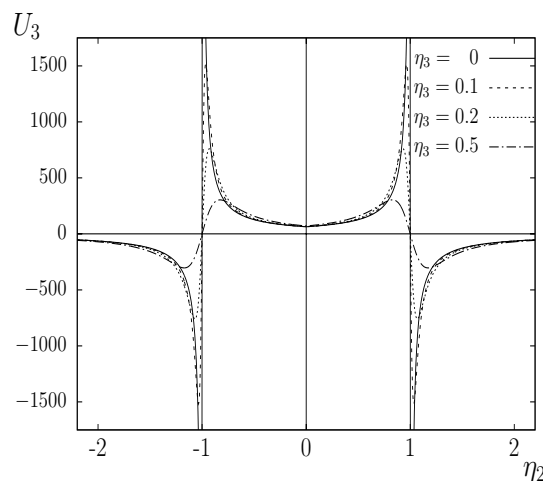


Figure 3.9. The scaled displacement U_3 vs. η_2 in the super-Rayleigh case for $\eta_1 = -1$.

The variation of the displacement U_3 along the other horizontal variable η_2 is depicted in Figure 3.9 for several values of the depth variable η_3 and $\eta_1 = -1$. Once again surface discontinuities similar to that in Figure 3.8 *b* are observed. However, here we have two surface discontinuities $\eta_2 = \pm\eta_1 = \pm 1$ due to structure of the displacement component u_3 , see equation (3.45).

The next Figure, Figure 3.10, shows the behaviour of the principal in-plane displacement U_1 . In this case, as in Figure 3.8, there are surface discontinuities at $\eta_1 = 0$ and $\eta_1 = -1$ respectively. It can again be observed that due to the causality principle there are no disturbances in front of the load.

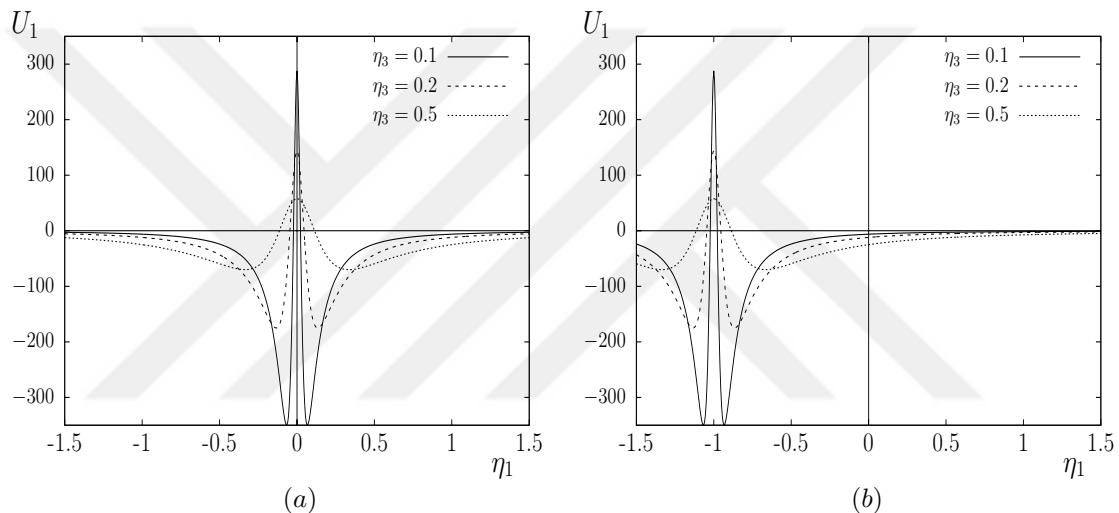


Figure 3.10. The scaled displacement U_1 vs. η_1 in the super-Rayleigh case for (a) $\eta_2 = 0$, (b) $\eta_2 = -1$.

Let us now consider the sub-Rayleigh case. In this case the speed of the load is $c = 0.9148c_2$ which corresponds to $c < c_R$ and again to $\varepsilon = 0.1$.

Figure 3.11 shows a typical variation of the vertical displacement along the horizontal variable η_2 at a given depth. The approximate formula (3.68) dictates a non-harmonic behaviour near the surface which may be seen through the curves for $\eta_3 = 0, 1, 3$ and 5 .

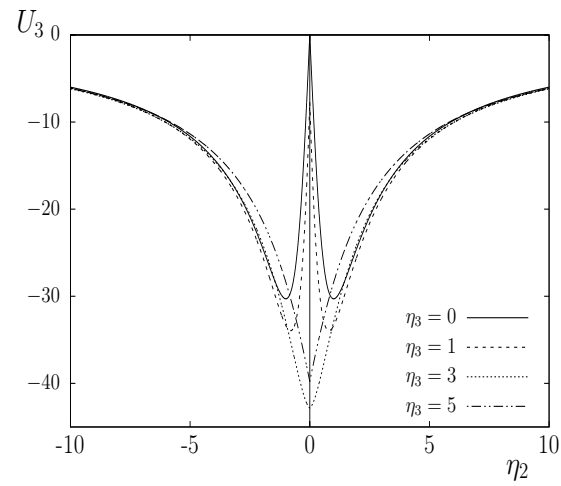


Figure 3.11. The scaled displacement U_3 vs. η_2 in the sub-Rayleigh case for $\eta_1 = 1$.

4. 3-DIMENSIONAL MOVING LOAD PROBLEM FOR A COATED ELASTIC HALF-SPACE

In this chapter the near-resonant regimes of a moving load in a 3D problem for a coated elastic half-space is considered. First, the statement of the problem is presented and then the problem is reduced to the steady-state regime by proposing two asymptotic scalings. The solutions of the reduced problems may be expressed through integral transforms. The evaluation of the obtained integrals are subject to asymptotic analysis in the far-field using the stationary phase method. Finally, numerical comparisons of exact and asymptotic results are presented for both cases.

4.1. Statement of the Problem and Scaling

Consider the 3D elastodynamic response of a linearly isotropic half-space ($-\infty < x_1, x_2 < \infty, 0 \leq x_3$) coated by a thin layer ($-\infty < x_1, x_2 < \infty, -h \leq x_3 \leq 0$) under the action of a concentrated vertical force of magnitude P moving at a constant speed c along the line $x_2 = 0$ on the surface $x_3 = -h$, see Figure 4.1.

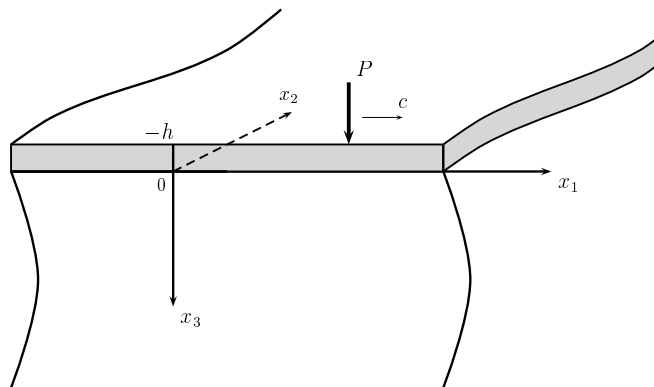


Figure 4.1. Coated half-space under a moving load.

The approximate hyperbolic-elliptic formulation will again be employed for the Rayleigh wave field. As a result of this approximation, analogous to the uncoated problem, we obtain the same elliptic equations given by (3.4) in the interior of the elastic half-space, which are

$$\frac{\partial^2 \varphi}{\partial x_3^2} + k_1^2 \Delta_2 \varphi = 0, \quad \frac{\partial^2 \psi_i}{\partial x_3^2} + k_2^2 \Delta_2 \psi_i = 0, \quad (i = 1, 2).$$

Due to the coating, however, boundary equation along the surface $x_3 = 0$ is now governed by the singularly perturbed hyperbolic equation

$$\Delta_2 \varphi - \frac{1}{c_R^2} \frac{\partial^2 \varphi}{\partial t^2} - bh \sqrt{-\Delta_2} \Delta_2 \varphi = AP \delta(x_1 - ct) \delta(x_2), \quad (4.1)$$

where b is a constant depending on the material parameters of the half-space and coating, A is defined by (2.90) and $\sqrt{-\Delta_2}$ is a pseudo-differential operator, for more details see [20], [21] and [14]. It is also worth mentioning that the parameter b in the proposed model may take both positive and negative values corresponding to the local minimum and maximum of the phase speed equal to Rayleigh wave speed, see [31], and also [14]. Therefore the sign of b is crucial for the type of the surface behaviour.

The approximate solution of the Rayleigh wave field for the coated elastic half-space can be obtained in a similar way to the uncoated problem from the solution of the sub-problems including 2D boundary value problems given by (3.4) and (4.1). Then the obtained solution may be extended over the interior of the half space by employing the Poisson formula. But here instead of this procedure, we will only deal with tangential displacements along the plane $x_3 = 0$. Using the displacement components introduced in (3.42₁)

$$u_1 = \frac{\partial \varphi}{\partial x_1} - \frac{\partial \psi_1}{\partial x_3}, \quad u_2 = \frac{\partial \varphi}{\partial x_2} - \frac{\partial \psi_2}{\partial x_3},$$

and the relations between the potentials on the surface $x_3 = 0$

$$\frac{\partial \varphi}{\partial x_i} = \frac{2}{1 + k_2^2} \frac{\partial \psi_i}{\partial x_3}, \quad i = 1, 2,$$

we obtain the expressions of the tangential displacements as

$$u_i = \frac{c_R^2}{2c_2^2} \frac{\partial \varphi}{\partial x_i}, \quad i = 1, 2. \quad (4.2)$$

In investigating the solution of equation (4.1) we restrict ourselves to the steady state regime. On introducing the moving coordinate $\lambda = x_1 - ct$, we get from

equation (4.1) for the sub-Rayleigh case

$$\frac{\partial^2 \varphi}{\partial x_2^2} - \varepsilon^2 \frac{\partial^2 \varphi}{\partial \lambda^2} - bh \sqrt{-\left(\frac{\partial^2}{\partial x_2^2} + \frac{\partial^2}{\partial \lambda^2}\right)} \left(\frac{\partial^2 \varphi}{\partial x_2^2} + \frac{\partial^2 \varphi}{\partial \lambda^2}\right) = AP \delta(\lambda) \delta(x_2), \quad (4.3)$$

and the super-Rayleigh case

$$\frac{\partial^2 \varphi}{\partial x_2^2} + \varepsilon^2 \frac{\partial^2 \varphi}{\partial \lambda^2} - bh \sqrt{-\left(\frac{\partial^2}{\partial x_2^2} + \frac{\partial^2}{\partial \lambda^2}\right)} \left(\frac{\partial^2 \varphi}{\partial x_2^2} + \frac{\partial^2 \varphi}{\partial \lambda^2}\right) = AP \delta(\lambda) \delta(x_2), \quad (4.4)$$

where ε is defined as in equation (3.8):

$$\varepsilon = \sqrt{\left|1 - \frac{c^2}{c_R^2}\right|}.$$

The adapted model is oriented to the analysis of a near-resonant response dominated by the Rayleigh wave contribution and is valid provided that $\varepsilon \ll 1$, see [15], [28]. It also assumes that the thickness of the coating h is small compared to a typical wavelength. The presence of two small parameters, namely ε and h , in equations (4.3) and (4.4) leads to two different types of degeneration; at $\varepsilon = 0$ and at $h = 0$, corresponding to the critical speed of the load coinciding with the Rayleigh wave speed, and an uncoated half-space, respectively. This observation motivates the scaling

$$\lambda = \frac{\xi bh}{\varepsilon^2}, \quad x_2 = \frac{\eta bh}{\varepsilon^3}, \quad (4.5)$$

which defines an elongated domain over the $(x_2 h^{-1}, \lambda h^{-1})$ plane, see Figure 4.2. Utilizing the scaling (4.5), equations (4.4) and (4.3) become

$$\frac{\partial^2 \varphi}{\partial \eta^2} - \frac{\partial^2 \varphi}{\partial \xi^2} - \sqrt{-\left(\frac{\partial^2}{\partial \xi^2} + \varepsilon^2 \frac{\partial^2}{\partial \eta^2}\right)} \left(\frac{\partial^2 \varphi}{\partial \xi^2} + \varepsilon^2 \frac{\partial^2 \varphi}{\partial \eta^2}\right) = \frac{AP}{\varepsilon} \delta(\xi) \delta(\eta), \quad (4.6)$$

and

$$\frac{\partial^2 \varphi}{\partial \eta^2} + \frac{\partial^2 \varphi}{\partial \xi^2} - \sqrt{-\left(\frac{\partial^2}{\partial \xi^2} + \varepsilon^2 \frac{\partial^2}{\partial \eta^2}\right)} \left(\frac{\partial^2 \varphi}{\partial \xi^2} + \varepsilon^2 \frac{\partial^2 \varphi}{\partial \eta^2}\right) = \frac{AP}{\varepsilon} \delta(\xi) \delta(\eta), \quad (4.7)$$

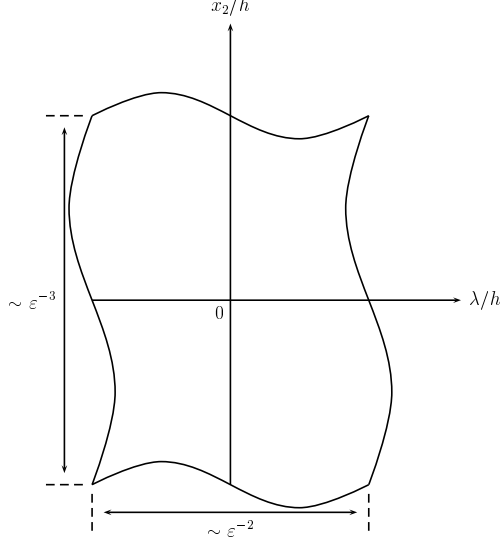


Figure 4.2. Asymptotic scaling.

respectively. Since ε is a small physical parameter, $O(\varepsilon^2)$ terms can be neglected. Neglecting $O(\varepsilon^2)$ terms in equations (4.6) and (4.7) we obtain

$$\frac{\partial^2 \varphi}{\partial \eta^2} - \frac{\partial^2 \varphi}{\partial \xi^2} - \sqrt{-\frac{\partial^2}{\partial \xi^2}} \frac{\partial^2 \varphi}{\partial \xi^2} = \frac{AP}{\varepsilon} \delta(\xi) \delta(\eta), \quad (4.8)$$

$$\frac{\partial^2 \varphi}{\partial \eta^2} + \frac{\partial^2 \varphi}{\partial \xi^2} - \sqrt{-\frac{\partial^2}{\partial \xi^2}} \frac{\partial^2 \varphi}{\partial \xi^2} = \frac{AP}{\varepsilon} \delta(\xi) \delta(\eta), \quad (4.9)$$

respectively.

4.2. Solution of the Problem

In this section we will obtain the solutions of the boundary equations (4.8) and (4.9), corresponding to sub and super-Rayleigh cases, respectively. The tangential displacements along the plane $x_3 = 0$ will then be expressed through the obtained solutions.

4.2.1. Super-Rayleigh case

Boundary equation (4.8) along the plane $x_3 = 0$ for the coated half-space, due to the inclusion of a term governed by a pseudo-differential operator, cannot be solved by means of the fundamental solution which was employed in Chapter 2. Therefore integral transform methods will be employed in order to obtain the solution of

equation (4.8). Hence, let us first apply the Fourier transform to equation (4.8) in the variable ξ . We know from Section 1.2 that the Fourier transform of the differential operator $L(\mathbf{x}, D)$ acting on the function $f(\mathbf{x})$ is equal to the symbol of the operator multiplied by $\hat{f}(\boldsymbol{\xi})$, the Fourier transform of $f(\mathbf{x})$. Since the symbol of $\sqrt{-\partial^2/\partial\xi^2}$ is $|k|$ the Fourier transform of equation (4.8) results in

$$\frac{d^2\varphi^F}{d\eta^2} + k^2(1 + |k|)\varphi^F = \frac{AP}{\varepsilon}\delta(\eta), \quad (4.10)$$

where

$$\varphi^F(k, \eta, 0) = \int_{-\infty}^{\infty} \varphi(\xi, \eta, 0) e^{-ik\xi} d\xi. \quad (4.11)$$

On applying two sided Laplace transform to (4.10) gives

$$\varphi^{FL} = \frac{AP}{\varepsilon} \frac{1}{s^2 + k^2(1 + |k|)}, \quad (4.12)$$

where

$$\varphi^{FL}(k, \eta, 0) = \int_{-\infty}^{\infty} \varphi^F(k, \eta, 0) e^{-s\eta} d\eta. \quad (4.13)$$

Taking into account the symmetry of the problem in the variable η , the inverse Laplace transform of equation (4.12), which can be evaluated through the residue calculus, may be expressed as

$$\varphi^F = \frac{AP}{\varepsilon} \frac{\sin\left(|k|\sqrt{1+|k|}|\eta|\right)}{|k|\sqrt{1+|k|}}. \quad (4.14)$$

Then the related inverse Fourier transform of equation (4.14) is written in integral form as

$$\varphi(\xi, \eta, 0) = \frac{AP}{2\pi\varepsilon} \int_{-\infty}^{\infty} \frac{\sin\left(|k|\sqrt{1+|k|}|\eta|\right)}{k\sqrt{1+k}} e^{ik\xi} dk. \quad (4.15)$$

Since the integrand of (4.15) is even, we may rewrite it as

$$\begin{aligned}
\varphi(\xi, \eta, 0) &= \frac{AP}{\pi\varepsilon} \int_0^\infty \frac{\sin(k\sqrt{1+k}|\eta|) \cos(k|\xi|)}{k\sqrt{1+k}} dk \\
&= \frac{AP}{2\pi\varepsilon} \int_0^\infty \frac{\sin(k\sqrt{1+k}|\eta| + k|\xi|) + \sin(k\sqrt{1+k}|\eta| - k|\xi|)}{k\sqrt{1+k}} dk \\
&= \frac{AP}{2\pi\varepsilon} \operatorname{Im} \left\{ \int_0^\infty \frac{e^{i(k\sqrt{1+k}|\eta| + k|\xi|)} + e^{i(k\sqrt{1+k}|\eta| - k|\xi|)}}{k\sqrt{1+k}} dk \right\}. \tag{4.16}
\end{aligned}$$

The tangential displacements given by (4.2) along the surface $x_3 = 0$ may now be expressed through the integral (4.16). Since the analysis is rather similar for both displacements we only deal with the horizontal displacement u_1 which can be written in the new variable as

$$u_1 = \frac{\varepsilon^2 c_R^2}{2bh c_2^2} \frac{\partial \varphi}{\partial \xi}. \tag{4.17}$$

Therefore u_1 is written from equation (4.16) as

$$u_1(\xi, \eta, 0) = \frac{AP c_R^2 \varepsilon \operatorname{sgn}(\xi)}{4\pi b h c_2^2} \sum_{n=1}^2 I_n(\xi, \eta), \tag{4.18}$$

where

$$I_n = (-1)^{n+1} \int_0^\infty \frac{\cos(|\xi| h_n(k))}{g(k)} dk = (-1)^{n+1} \operatorname{Re} \int_0^\infty \frac{e^{i|\xi| h_n(k)}}{g(k)} dk, \quad n = 1, 2 \tag{4.19}$$

and

$$g(k) = \sqrt{1+k}, \quad h_n(k) = k [g(k)\mu - (-1)^n], \quad \mu = \left| \frac{\eta}{\xi} \right|. \tag{4.20}$$

Calculation of integrals (4.19) in the conventional methods is quite difficult even almost impossible. Therefore we will investigate the far-field asymptotic behaviour of the oscillating integrals (4.19) as $|\xi| \gg 1$, assuming $\mu \sim 1$. In other words we try to obtain an asymptotic expansion of the integral for large values of ξ . To this end, we make use of stationary phase method which gives an asymptotic expansion of integrals when the integrand has stationary points in the interval of the integral, see Section 1.6.4.

We first investigate the asymptotic behaviour of I_1 where $h_1(k)$ is defined in equation (4.20). The stationary points of $h_1(k)$ can be determined by its derivative, i.e.

$$h_1'(k) = \mu\sqrt{1+k} + \frac{k\mu}{2\sqrt{1+k}} + 1 = 0.$$

This equation can be put in an appropriate form by changing the variable $\rho^2 = 1+k$, giving

$$3\mu\rho^2 + 2\rho - \mu = 0,$$

whose roots are

$$\rho_1 = \frac{-1 + \sqrt{1 + 3\mu^2}}{3\mu} \quad \text{and} \quad \rho_2 = \frac{-1 - \sqrt{1 + 3\mu^2}}{3\mu}. \quad (4.21)$$

Because of the definition of ρ these new roots must be greater than one so that they can be a stationary point of I_1 . The second root ρ_2 , since $\mu = \left|\frac{\eta}{\xi}\right| > 0$, is negative and outside of the integration domain. Therefore ρ_2 is not a stationary point for the integral I_1 . Similarly since ρ_1 must be greater than one, we can write

$$\rho_1 = \frac{-1 + \sqrt{1 + 3\mu^2}}{3\mu} > 1.$$

It can be obtained from the last inequality that $2\mu^2 + 2\mu < 0$. However, since $\mu > 0$ this inequality cannot be satisfied. Therefore ρ_1 cannot be a stationary point of the investigated integral. Thus I_1 does not have any stationary points.

Let us now investigate the stationary points of the second integral I_2 where $h_2(k)$ is given by (4.20). The stationary points can be obtained by

$$h_2'(k) = \mu\sqrt{1+k} + \frac{k\mu}{2\sqrt{1+k}} - 1 = 0.$$

Changing the variable as $\rho^2 = 1+k$ gives

$$3\mu\rho^2 - 2\rho - \mu = 0,$$

the roots of which are given by

$$\rho_3 = \frac{1 + \sqrt{1 + 3\mu^2}}{3\mu}, \quad \text{and} \quad \rho_4 = \frac{1 - \sqrt{1 + 3\mu^2}}{3\mu}. \quad (4.22)$$

Since $\mu > 0$, the second root ρ_4 is less than unity and is not be a stationary point of the integral I_2 . As for the first root ρ_3 , requiring $\rho_3 > 1$, we have

$$\rho_3 = \frac{1 + \sqrt{1 + 3\mu^2}}{3\mu} > 1,$$

which gives $2\mu^2 - 2\mu < 0$. Therefore we see that I_2 has a stationary point when $0 < \mu < 1$ which is given by

$$k_* = \frac{2(1 - 3\mu^2 + \sqrt{1 + 3\mu^2})}{9\mu^2}. \quad (4.23)$$

There are two points to be noted. First, since the first integral I_1 does not have a stationary point whereas the second integral I_2 has a one, the effect of the first integral is asymptotically negligible compared to the second integral I_2 which is dominated by the contribution of the stationary point of $h_2(k)$. In order to obtain an approximate formulation for u_1 it is sufficient to find the asymptotic expansion of I_2 . Second, at the contour of the Mach cone $\mu = 1$ ($|\xi| = |\eta|$) the stationary point $k_* = 0$ coincides with the lower limit of the integral I_2 . It is also known that an integral has two different order of asymptotic expansions when the stationary point is inside or at the boundary of the integration domain. Therefore we have to apply the uniform stationary phase method in order to obtain a uniform asymptotic expansion for I_2 (see [32]).

Let us now expand $h_2(k)$ in a Taylor series about k_* of order 2 in order to get the uniform asymptotic expansion of I_2 . Since k_* is a stationary point of $h_2(k)$, $h_2'(k_*) = 0$. Therefore the Taylor expansion of $h_2(k)$ is written as

$$h_2(k) = h_2(k_*) + \frac{h_2''(k_*)}{2}(k - k_*)^2.$$

Hence, if we apply the uniform stationary phase method and take the leading order term, we have

$$I_2 \sim \operatorname{Re} \left\{ \frac{e^{i|\xi|h_2(k_*)}}{g(k_*)} \int_0^\infty e^{\frac{1}{2}i|\xi|h_2''(k_*)(k-k_*)^2} dk \right\}, \quad (4.24)$$

where

$$h_* = h_2(k_*) = \frac{2(1 - 3\mu^2 + \sqrt{1 + 3\mu^2})(\sqrt{1 + 3\mu^2} - 2)}{27\mu^2}, \quad (4.25)$$

$$h_*'' = h_2''(k_*) = \frac{9\mu^2(1 + 3\mu^2 + \sqrt{1 + 3\mu^2})}{2(1 + \sqrt{1 + 3\mu^2})}, \quad (4.26)$$

and

$$g_* = g(k_*) = \frac{1 + \sqrt{3\mu^2 + 1}}{3\mu}. \quad (4.27)$$

Introducing the variable u

$$\sqrt{|\xi| \frac{h_*''}{2}}(k - k_*) = u$$

the asymptotic expression of I_2 given by (4.24) may be written as

$$\begin{aligned} I_2 &\sim \operatorname{Re} \left\{ \frac{e^{i|\xi|h_*}}{g_*} \sqrt{\frac{2}{|\xi|h_*''}} \int_{-k_*\sqrt{\frac{|\xi|h_*''}{2}}}^\infty e^{iu^2} du \right\} \\ &\sim \operatorname{Re} \left\{ \frac{e^{i|\xi|h_*}}{g_*} \sqrt{\frac{2}{|\xi|h_*''}} \left[\sqrt{\frac{\pi}{8}} - C \left(-k_*\sqrt{\frac{|\xi|h_*''}{2}} \right) + \right. \right. \\ &\quad \left. \left. + i \left(\sqrt{\frac{\pi}{8}} - S \left(-k_*\sqrt{\frac{|\xi|h_*''}{2}} \right) \right) \right] \right\}, \quad (4.28) \end{aligned}$$

where $S(x)$ and $C(x)$ are the Fresnel functions, defined by

$$S(x) = \int_0^x \sin(t^2) dt, \quad C(x) = \int_0^x \cos(t^2) dt, \quad (4.29)$$

see [33]. Taking the real part of (4.28) we obtain the asymptotic expansion of I_2 as

$$I_2 \sim \frac{1}{g_*} \sqrt{\frac{2}{|\xi| h_*''}} \left\{ \cos(|\xi| h_*) \left[\sqrt{\frac{\pi}{8}} - C \left(-k_* \sqrt{\frac{|\xi| h_*''}{2}} \right) \right] - \right. \\ \left. - \sin(|\xi| h_*) \left[\sqrt{\frac{\pi}{8}} - S \left(-k_* \sqrt{\frac{|\xi| h_*''}{2}} \right) \right] \right\}. \quad (4.30)$$

The resulting displacement u_1 is then given by

$$u_1 \sim \frac{AP \varepsilon c_R^2 \operatorname{sgn}(\xi)}{4\pi b h c_2^2 g_*} \sqrt{\frac{2}{h_*''}} \frac{1}{|\xi|^{1/2}} F(|\xi|, \mu), \quad (4.31)$$

where

$$F(|\xi|, \mu) = \cos(|\xi| h_*) \left[\frac{\pi}{8} - C \left(-k_* \sqrt{\frac{|\xi| h_*''}{2}} \right) \right] - \\ - \sin(|\xi| h_*) \left[\frac{\pi}{8} - S \left(-k_* \sqrt{\frac{|\xi| h_*''}{2}} \right) \right]. \quad (4.32)$$

The interpretation of the formulae in this section written in terms of $|\xi|$ and $|\eta|$ relies on the implementation of the causality principle. In the absence of a coating, when $h = 0$, equation (4.8) degenerates to the wave equation. When the half-space is coated on its surface it is logical to deal with the Mach cones behind the load only, i.e. at $b > 0$ for $\xi > 0$ and $b < 0$ for $\xi < 0$, as follows from scaling (4.5), see Figure 4.3.

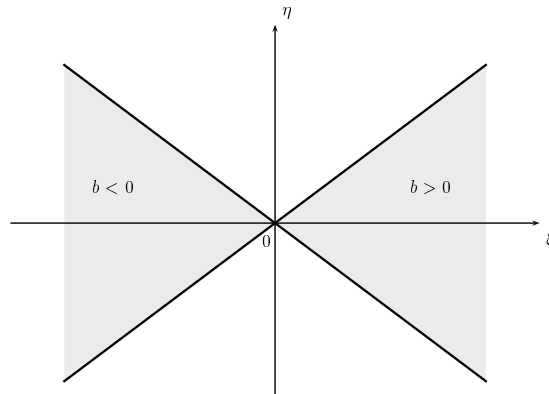


Figure 4.3. Mach cone in coated half-space.

The full solution of the associated original problem in 3D elasticity will contain the contribution of the faster compression and shear waves ignored within the framework of the adapted specialized formulation (cf. Section 3.1). As a result, the question of taking into consideration both Mach cones (behind and in front of the load) may be raised. To a certain extent, this may be relevant to the phenomenon of a head shear wave propagating faster than a cylindrical shear wave in case of the plane Lamb problem (cf. [34]).

Another interesting feature is concerned with the dispersive nature of the analyzed surface wave governed by a singularly perturbed wave equation. In this case, due to causality, we seemingly have to require the decay of the solution outside the interior of the Mach cones predicted by the related degenerate non-dispersive equation. The asymptotic behaviours of the Fresnel functions in equation (4.32) at the large imaginary values of the argument show that the function (4.32) is exponentially small at $\mu - 1 \gg |\xi|^{-1}$.

4.2.2. Sub-Rayleigh case

In this section, we will obtain an asymptotic solution of the longitudinal displacement u_1 in the sub-Rayleigh case. To this end, we will employ the integral transforms to obtain the solution of the boundary equation (4.9) as was done in the previous section. Taking, first, the Fourier transform of equation (4.9) in the variable ξ , we get

$$\frac{d^2\varphi^F}{d\eta^2} - k^2(1 - |k|)\varphi^F = \frac{AP}{\varepsilon}\delta(\eta), \quad (4.33)$$

where Fourier transform is defined by (4.11). Applying the two-sided Laplace transform defined by (4.13) to equation (4.33) results in

$$\varphi^{FL} = \frac{AP}{\varepsilon} \frac{1}{s^2 - k^2(1 - |k|)}. \quad (4.34)$$

Taking into account the structure of the investigated problem, it is a fact that the solution of equation (4.34) must be symmetric in η and vanishes as $\eta \rightarrow \infty$.

Therefore the inverse Laplace transform of (4.34) may be written as

$$\varphi^F(k, \eta, 0) = \begin{cases} -\frac{AP}{\varepsilon} \frac{e^{-|k|\sqrt{1-|k}|\eta}}{2|k|\sqrt{1-|k}|}, & |k| < 1; \\ \frac{AP}{\varepsilon} \frac{\sin\left(|k|\sqrt{|k|-1}|\eta\right)}{|k|\sqrt{|k|-1}}, & |k| > 1. \end{cases} \quad (4.35)$$

The inverse Fourier transform of equation (4.35) may be written in the usual manner, however due to the singularities of the integrand, we will write the inverse transform in three parts giving

$$\begin{aligned} \varphi(\xi, \eta, 0) &= \frac{AP}{2\pi\varepsilon} \left\{ \int_{-\infty}^{-1} \frac{\sin(-k\sqrt{-k-1}|\eta|)}{-k\sqrt{-k-1}} e^{ik\xi} dk - \int_{-1}^1 \frac{e^{-|k|\sqrt{1-|k}|\eta}}{|k|\sqrt{1-|k}|} e^{ik\xi} dk + \right. \\ &\quad \left. + \int_1^{\infty} \frac{\sin(k\sqrt{k-1}|\eta|)}{k\sqrt{k-1}} e^{ik\xi} dk \right\} \\ &= \frac{AP}{2\pi\varepsilon} \left\{ \int_1^{\infty} \frac{\sin(k\sqrt{k-1}|\eta|)}{k\sqrt{k-1}} e^{-ik\xi} dk - 2 \int_0^1 \frac{e^{-k\sqrt{1-k}|\eta|}}{k\sqrt{1-k}} \cos(k\xi) dk + \right. \\ &\quad \left. + \int_1^{\infty} \frac{\sin(k\sqrt{k-1}|\eta|)}{k\sqrt{k-1}} e^{ik\xi} dk \right\} \\ &= \frac{AP}{2\pi\varepsilon} \left\{ \int_1^{\infty} \frac{\sin(k\sqrt{k-1}|\eta|)}{k\sqrt{k-1}} (e^{ik\xi} + e^{-ik\xi}) dk - 2 \int_0^1 \frac{e^{-k\sqrt{1-k}|\eta|}}{k\sqrt{1-k}} \cos(k\xi) dk \right\} \\ &= \frac{AP}{\pi\varepsilon} \left\{ \int_1^{\infty} \frac{\sin(k\sqrt{k-1}|\eta|)}{k\sqrt{k-1}} \cos(k|\xi|) dk - \int_0^1 \frac{e^{-k\sqrt{1-k}|\eta|}}{k\sqrt{1-k}} \cos(k\xi) dk \right\}. \quad (4.36) \end{aligned}$$

Thus, the longitudinal displacement u_1 along the plane $x_3 = 0$ can be expressed by

$$\begin{aligned} u_1(\xi, \eta, 0) &= \frac{AP\varepsilon c_R^2 \operatorname{sgn}(\xi)}{2\pi c_2^2 bh} \left[\int_0^1 \frac{e^{-k\sqrt{1-k}|\xi|\mu}}{\sqrt{1-k}} \sin(k|\xi|) dk - \right. \\ &\quad \left. - \int_1^{\infty} \frac{\sin(k\sqrt{k-1}|\xi|\mu)}{\sqrt{k-1}} \sin(k|\xi|) dk \right]. \quad (4.37) \end{aligned}$$

Let us investigate asymptotic expansion ($|\xi| \gg 1$) of the integral (4.37). We begin with the first integral in equation (4.37). Changing the variable k to $r = \sqrt{1-k}$, the integral takes the form

$$\int_0^1 \frac{e^{-k\sqrt{1-k}} \mu |\xi|}{\sqrt{1-k}} \sin(k\xi) dk = 2 \int_0^1 e^{|\eta|(r^2-1)r} \sin((1-r^2)|\xi|) dr. \quad (4.38)$$

Riemann-Lebesgue lemma dictates that the integral (4.38) approaches zero as $\xi \rightarrow \infty$, since the integrand is a product of an integrable function, even differentiable with respect to the variable r , and a rapidly oscillating sine term. This approach is as fast as the order of the derivative and therefore faster than any power of $1/|\xi|$.

As for the second integral of (4.37), we need to apply the stationary phase method. If the integrand has stationary points then the leading term of the asymptotic expansion will behave like $1/|\xi|^{1/2}$. We begin by writing the second integral of (4.37) in the form

$$\int_1^\infty \frac{\sin(k\sqrt{k-1}|\xi|\mu)}{\sqrt{k-1}} \sin(k|\xi|) dk = \frac{1}{2} \operatorname{Re} \left\{ \int_1^\infty \frac{e^{i|\xi|(k\sqrt{k-1}\mu-k)}}{\sqrt{k-1}} dk - \int_1^\infty \frac{e^{i|\xi|(k\sqrt{k-1}\mu+k)}}{\sqrt{k-1}} dk \right\}, \quad (4.39)$$

where μ is again defined as $\mu = \left| \frac{\eta}{\xi} \right|$. Changing variable k to $t = \sqrt{k-1}$, the integrals in equation (4.39) become

$$\begin{aligned} \int_1^\infty \frac{\sin(k\sqrt{k-1}|\xi|\mu)}{\sqrt{k-1}} \sin(k|\xi|) dk &= \\ &= \operatorname{Re} \left\{ \int_0^\infty e^{i|\xi|(t^2+1)(t\mu-1)} dt - \int_0^\infty e^{i|\xi|(t^2+1)(t\mu+1)} dt \right\}. \end{aligned} \quad (4.40)$$

We write

$$p_1(t) = (t^2 + 1)(t\mu - 1), \quad p_2(t) = (t^2 - 1)(t\mu + 1), \quad (4.41)$$

which correspond to the exponents of the first and second integrands on the right hand side of equation (4.40). The stationary points of the first integral in equation (4.40) are then found through the solutions of the following equation

$$p_1'(t) = 3\mu t^2 - 2t + \mu = 0$$

as

$$t_1 = \frac{1 + \sqrt{1 - 3\mu^2}}{3\mu}, \quad t_2 = \frac{1 - \sqrt{1 - 3\mu^2}}{3\mu}. \quad (4.42)$$

In this case the roots are inside the integration domain for $0 < \mu < \frac{1}{\sqrt{3}}$. Similarly the stationary points of the second integral in (4.40) can be obtained from the solution of the equation

$$p_2'(t) = 3\mu t^2 + 2t + \mu = 0$$

as

$$t_3 = \frac{-1 + \sqrt{1 - 3\mu^2}}{3\mu}, \quad t_4 = \frac{-1 - \sqrt{1 - 3\mu^2}}{3\mu}. \quad (4.43)$$

These roots will not be in the domain of integration for any values of μ . Therefore the second integral does not have any stationary points.

Since asymptotic contribution of the first integral in (4.37) comes from the end points of the integral and only the first part of the second integral given in (4.40) has a stationary point, the leading order term of the asymptotic behaviour of the longitudinal displacement u_1 arises from the stationary point of the first integral in (4.40). Here the point to be noted is that these two roots coincide along the line $\mu = \frac{1}{\sqrt{3}}$ ($|\xi| = \sqrt{3}|\eta|$). This again motivates us to make use of the uniform stationary phase method. According to the uniform stationary phase method when two stationary points coincide in the domain of integration the integral is converted to Airy type integral and the asymptotic expansion of the integral can be obtained by using the asymptotic expansion of the Airy function which is defined as

$$\text{Ai}(z) = \frac{1}{\pi} \int_0^{\infty} \cos\left(\frac{t^3}{3} + zt\right) dt = \frac{1}{2\pi} \text{Re} \int_{-\infty}^{\infty} e^{i(t^3/3 + zt)} dt, \quad (4.44)$$

(see [33]). The first integral in (4.40) may be written as

$$\int_0^{\infty} e^{i|\xi|(t^2+1)(t\mu-1)} dt = \int_0^{\infty} e^{i|\xi|\mu(t^3-\frac{1}{\mu}t^2+t-\frac{1}{\mu})} dt. \quad (4.45)$$

The argument of the exponential function may be organized as

$$\begin{aligned} t^3 - \frac{1}{\mu}t^2 + t - \frac{1}{\mu} &= \left(t - \frac{1}{3\mu}\right)^3 - \frac{t}{3\mu^2} + \frac{1}{27\mu^3} + t - \frac{1}{\mu} \\ &= \left(t - \frac{1}{3\mu}\right)^3 + t - \frac{t}{3\mu^2} - \frac{1}{3\mu} + \frac{1}{9\mu^3} - \frac{2}{27\mu^3} - \frac{2}{3\mu} \\ &= \left(t - \frac{1}{3\mu}\right)^3 + t \left(1 - \frac{1}{3\mu^2}\right) - \frac{1}{3\mu} \left(1 - \frac{1}{3\mu^2}\right) - \frac{2}{3} \left(\frac{1}{\mu} - \frac{1}{9\mu^3}\right) \\ &= \left(t - \frac{1}{3\mu}\right)^3 + \left(1 - \frac{1}{3\mu^2}\right) \left(t - \frac{1}{3\mu}\right) - \frac{2}{3} \left(\frac{1}{\mu} - \frac{1}{9\mu^3}\right) \end{aligned}$$

hence it can be obtained from (4.40) that

$$\begin{aligned} \int_1^{\infty} \frac{\sin(k\sqrt{k-1}|\xi|\mu)}{\sqrt{k-1}} \sin(k|\xi|) dk &\sim \operatorname{Re} \int_0^{\infty} e^{i|\xi|\mu \left[\left(t - \frac{1}{3\mu}\right)^3 + \alpha \left(t - \frac{1}{3\mu}\right) + \beta \right]} dt \\ &= \operatorname{Re} \left\{ e^{i|\xi|\mu\beta} \int_0^{\infty} e^{i|\xi|\mu \left[\left(t - \frac{1}{3\mu}\right)^3 + \alpha \left(t - \frac{1}{3\mu}\right) \right]} dt \right\}, \end{aligned} \quad (4.46)$$

where

$$\alpha = \frac{3\mu^2 - 1}{3\mu^2}, \quad \beta = -\frac{2(9\mu^2 + 1)}{27\mu^3}. \quad (4.47)$$

Now changing the variable as

$$|\xi|\mu \left(t - \frac{1}{3\mu}\right)^3 = \frac{z^3}{3},$$

(4.46) takes the form

$$\begin{aligned} \int_1^{\infty} \frac{\sin(k\sqrt{k-1}|\xi|\mu)}{\sqrt{k-1}} \sin(k|\xi|) dk &\sim \operatorname{Re} \left\{ \frac{e^{i|\xi|\beta}}{\sqrt[3]{3|\xi|\mu}} \int_{-\frac{\sqrt[3]{3|\xi|\mu}}{3\mu}}^{\infty} e^{i\left(\frac{z^3}{3} + \frac{\alpha|\xi|\mu}{\sqrt[3]{3|\xi|\mu}}z\right)} dz \right\} \\ &\sim \frac{\cos(|\xi|\mu\beta)}{\sqrt[3]{3|\xi|\mu}} \int_{-\infty}^{\infty} \cos\left(\frac{z^3}{3} + \gamma z\right) dz - \frac{\sin(|\xi|\mu\beta)}{\sqrt[3]{3|\xi|\mu}} \int_{-\infty}^{\infty} \sin\left(\frac{z^3}{3} + \gamma z\right) dz, \end{aligned} \quad (4.48)$$

where

$$\gamma = \frac{\alpha|\xi|\mu}{\sqrt[3]{3|\xi|\mu}} = \frac{3\mu^2 - 1}{(3\mu)^{4/3}} |\xi|^{2/3}. \quad (4.49)$$

Here the second integral in (4.48) will be zero since $\sin\left(\frac{z^3}{3} + \gamma z\right)$ is an odd function with respect to z . Thus, taking into account the asymptotic expansion of the Airy function the asymptotic expansion of the investigated integral may be written from equation (4.48) as

$$\int_1^{\infty} \frac{\sin(k\sqrt{k-1}|\xi|\mu)}{\sqrt{k-1}} \sin(k|\xi|) dk \sim \frac{2\pi}{\sqrt[3]{3|\xi|\mu}} \cos(|\xi|\mu\beta) \operatorname{Ai}(\gamma). \quad (4.50)$$

Hence, substitution of formula (4.50) into (4.37) results in the far-field asymptotic expansion for the longitudinal displacement u_1 as

$$u_1 \sim -\frac{AP \varepsilon c_R^2 \operatorname{sgn}(\xi)}{c_2^2 b h \sqrt[3]{3|\xi|\mu}} \cos(|\xi|\mu\beta) \operatorname{Ai}(\gamma). \quad (4.51)$$

4.3. Numerical Results for the Coated Half-Space

We now investigate the accuracy of the asymptotic solutions of the longitudinal displacement u_1 along the plane $x_3 = 0$, which are expressed by equations (4.31) and (4.51) for the super and sub-Rayleigh cases respectively. To this end, we will compare numerically the approximate and exact solutions. A numerical integration scheme will be employed to obtain the numerics for the exact solution.

In the super-Rayleigh case, the longitudinal displacement u_1 will be scaled as

$$U_1 = \frac{4\pi b h c_2^2}{AP c_R^2 \varepsilon} u_1, \quad (4.52)$$

and we present numerical illustrations of the scaled displacement, which contain longitudinal and transverse cross-sections of the profiles, respectively. On these plots, the results of the numerical integration of equation (4.18) are depicted by solid lines with the dotted line corresponding to the asymptotic approximation (4.31). The first figure, Figure 4.4, shows the dependence of U_1 on the transverse variable $|\eta|$, where the calculations are performed for the value of $|\xi| = 5$. The second figure, Figure 4.5, depicts the variation of U_1 on $|\xi|$ for $|\eta| = 5$.

We clearly see, from Figures 4.4 and 4.5, that dispersive effect of the coating smoothes out the discontinuities appearing along the lines $|\xi| = |\eta|$ in the uncoated half-space problem (see Section 2.4). The oscillations occur within the Mach cone, decaying away from it. The periods of the oscillations diminish on both graphs as $\mu \rightarrow 0$, due to $h_* \rightarrow \infty$, as may be noticed from equation (4.25).

The asymptotic formula (4.31) provides a surprisingly accurate approximation of the solution (4.18), which is applicable even at not very large values of the parameter $|\xi|$, used on Figures 4.4 and 4.5. This is due to the argument of the Fresnel functions $-k_* \sqrt{\frac{|\xi|h_*'}{2}} \sim |\xi|^{1/2} \mu^{-1}$ in equation (4.32), therefore we actually operate with a larger parameter $|\xi| \mu^{-2}$.

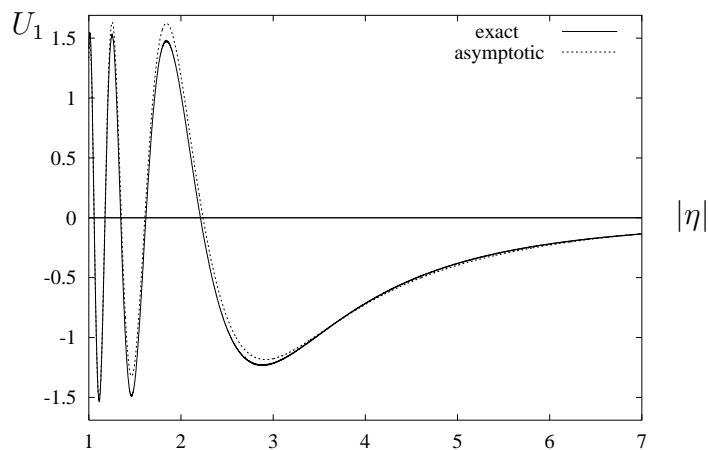


Figure 4.4. Profile of the super-Rayleigh displacement U_1 at $|\xi| = 5$.

In order to provide a better overview of the investigated wave phenomena, we present a 3D illustration of a part of the scaled displacement profile, corresponding to the exact integral in equation (4.18) (cf. 4.6).

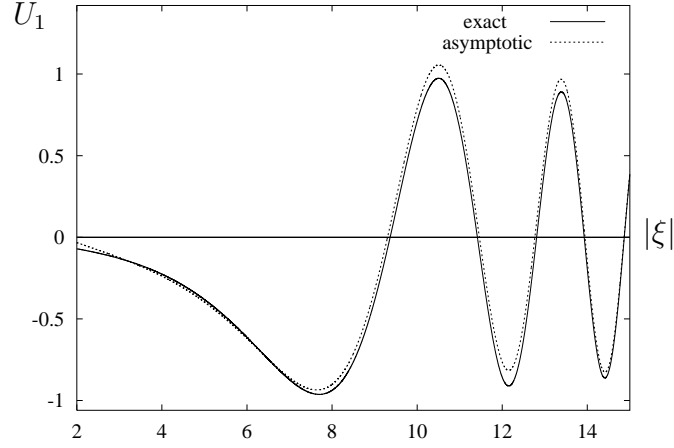


Figure 4.5. Profile of the super-Rayleigh displacement U_1 at $|\eta| = 5$.

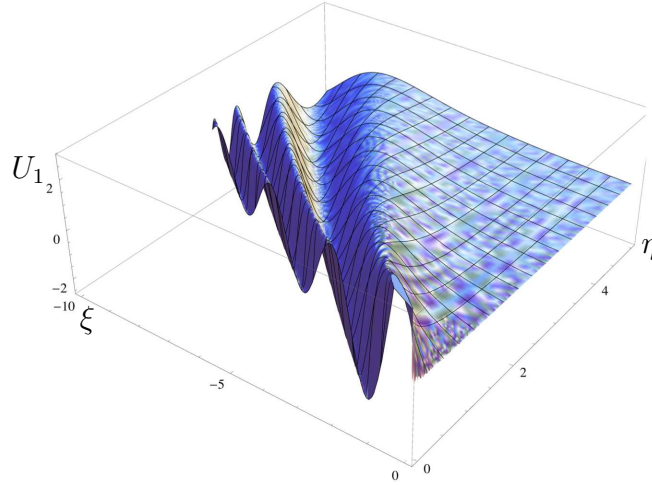


Figure 4.6. A 3D profile of the longitudinal super-Rayleigh displacement U_1 .

In the sub-Rayleigh case, similarly, we present scaled longitudinal displacement as

$$U_1 = \frac{bhc_2^2}{APc_R^2\varepsilon}u_1, \quad (4.53)$$

and comparisons of the scaled exact solution, equation (4.37), and far-field asymptotic approximation, equation (4.51), are illustrated. In the illustrations the solid and dotted lines correspond to the exact and asymptotic solutions respectively.

The calculations for Figure 4.7 are performed for a fixed value of $|\eta| = 5$ and in Figure 4.8 a perpendicular cross-section at $|\xi| = 10$ are depicted. It may be observed from Figures 4.7 and 4.8 that even though there is no Mach cone in the sub-Rayleigh case, there is still a region of oscillations associated with $\mu < \frac{1}{\sqrt{3}}$. The period of

the oscillations decreases as $\mu \rightarrow 0$. In the region $\mu > \frac{1}{\sqrt{3}}$ the profile demonstrates exponential decay.

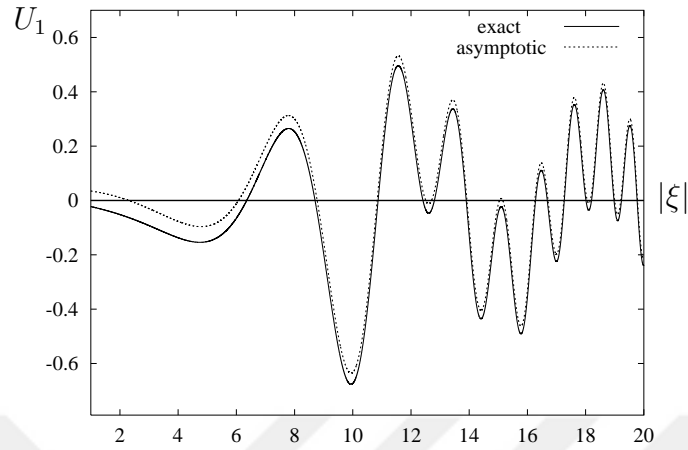


Figure 4.7. Transverse cross-section of the sub-Rayleigh displacement profile U_1 at $|\eta| = 5$.

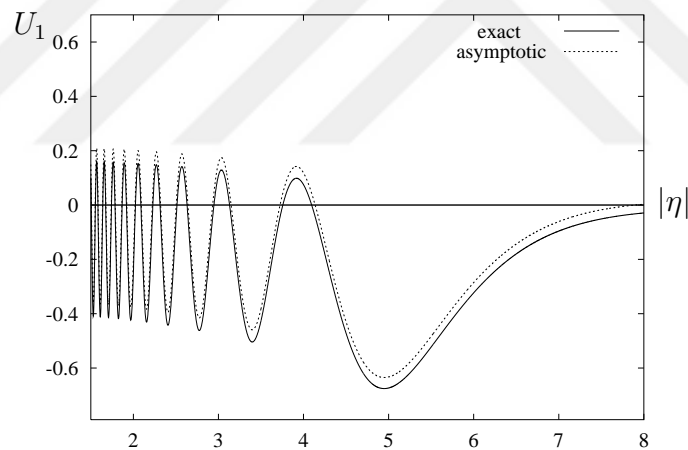


Figure 4.8. Longitudinal cross-section of the sub-Rayleigh displacement profile U_1 at $|\xi| = 10$.

Concluding this section, we present a 3D numerical illustration of the scaled displacement U_1 defined in equation (4.53) over the region $-10 \leq \xi \leq 10$, $0 \leq \eta \leq 5$, see Figure 4.9.

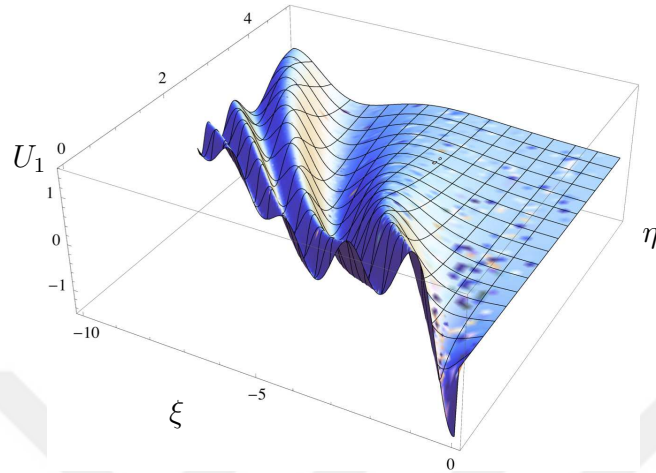


Figure 4.9. A 3D profile of the longitudinal sub-Rayleigh displacement U_1 .

5. CONCLUSIONS

This thesis is mainly concerned about the dynamical effects associated with the Rayleigh wave, in particular the stationary and resonance effects of moving loads on elastic and coated elastic half-spaces. The problems tackled make use of an asymptotic model, described in Chapter 2, aimed at deriving only the surface wave contributions on linear elastic solids, with a potential of extending its applicability to bodies with more complicated geometries and physical properties. The method relies on a certain scaling depending on the load speed as well as relating the wave potentials on the surface of the elastic solid so as to reduce the dimension of the problem. Such a relation among the potentials was first derived by Chadwick in his well known work on surface and interfacial waves (see, [8]). Two problems are therefore considered employing the mentioned method.

In Chapter 3, a 3D mathematical model of the dynamical effects of a load moving on the surface of a linear, isotropic elastic half-space is considered. The problem is reduced to a hyperbolic equation on the surface and two elliptic equations in the interior of the elastic half-space due to the application of the aforementioned asymptotic model. An approximate solution is then obtained, to the best of author's knowledge, for the first time in terms of elementary functions. The accuracy of the solution depends on the scaling, i.e. the small parameter of the problem defined in terms of the difference between the load speed and the Rayleigh one, signifying a near-field solution. The asymptotic model also reveals important advantages for the Rayleigh wave. The simple explicit formulae for transient displacement, derived via the asymptotic model, provide simpler analysis of the problem for given loads and stresses. The formulations for the displacement make available a better interpretation of the surface wave and also show that the considered problem has not much in common with its 2D counterpart. First of all, the 3D treatment reveals a clear distinction between the sub and super-Rayleigh cases which is not a feature of a more traditional plane strain problem. As an example the discontinuities along a straight line on the surface characteristic of the 3D super-Rayleigh case are discussed. It is remarkable that in the super-Rayleigh case these discontinuities appear only behind of the load because of the causality principle. At the end of Chapter 3 the transient

surface motion is tackled. Asymptotic consideration of the transient surface motion enables one to determine the rate of growth in time at the resonant Rayleigh wave speed. It is shown that there is an extra time-dependent logarithmic term in the surface solution which is homogenous over the surface and as a consequence, does not affect the displacement.

Chapter 4 examines the dynamics of a coated half-space under the action of a point load moving steadily along the surface of the half-space. The reduction of the 3D mathematical model to a pair of 2D plane problems is achieved, again, through the use of the small parameter of the previous Chapter. The model enables the simplification of all the derivations significantly, due to ignoring the contribution of compression and shear bulk waves. In addition, the considered model provides a more straightforward qualitative insight, including, for example, discussion of the causality principle in the application to a dispersive wave. The asymptotic model, again, reveals two different kind of surface equations depending on the relation between the load and Rayleigh wave speeds. Scaling, taking into consideration the degeneration characteristics of the near-resonant regimes and the small thickness of the coating, is considered. Unlike the uncoated half-space, however, certain difficulties arises due to the thin coating resulting in a pseudo-differential equation on the surface. The presence of the pseudo-differential operator prevents obtaining the solution in terms of simple functions. Therefore the solutions of the 2D scaled equations governing the surface motion are derived for both sub and super-Rayleigh cases in terms of integrals which require the techniques of asymptotic integration such as the method of stationary phase, etc. The associated wave field over the interior, similar the uncoated case, can be relatively easily restored by solving analytically or numerically the standard boundary value problems for pseudo-static elliptic equations. Thus the results obtained for the surface motion are expressed through the Airy function and Fresnel integrals. These integral representations can be useful for investigating the transition regions along the surface. For the super-Rayleigh case such a region is associated with the contour of the Mach cone. As might be expected, the presence of the coating results in smoothing of the singularities arising in the corresponding problem for the uncoated half-space.

The proposed approach may be generalized to media with more sophisticated

properties incorporating the effects of pre-stress, anisotropy, layered structure, viscosity as well as mixed problems for travelling stamps and cracks. There is also an obvious potential for a further insight into transient dynamics exploiting a key role of the Rayleigh wave in modelling of a scalar wave equation specified on the surface. In particular, there is a possibility for studying the accelerating sources similar to what has been recently done in acoustics, see [35]. The derived model for the coated half-space may, also, be extended to linear surface waves in case of anisotropic and pre-stress coatings.



REFERENCES

- [1] Love, A. E. H. (1944). A treatise on the mathematical theory of elasticity. New York: Dover Publications.
- [2] Strutt, J. W. (1885). On waves propagated along the plane surface of an elastic solid. *Proc. Lond. Math. Soc.*, 17, 4-11.
- [3] Love, A. E. H. (1911). Some problems of geodynamics. Cambridge University Press.
- [4] Lamb, H. (1917). On waves in an elastic plate. *Proc. R. Soc. Lond., Ser. A*, 93, 376-384.
- [5] Stoneley, R. (1924). Elastic waves at the surface of separation of two solids. *Proc. R. Soc. Lond., A*, 106, 376-384.
- [6] Scholte, J. G. (1947). The range and existence of Rayleigh and Stoneley waves. *Geophysical Journal International*, 5(s5), 120-126.
- [7] Friedlander, F. G. (1948). On the total reflection of plane waves. *Quart. J. Mech. Appl. Math*, 1, 376-384.
- [8] Chadwick, P. (1976). Surface and interfacial waves of arbitrary form in isotropic elastic media. *J. Elast*, 6, 73-80.
- [9] P. Kiselev, A. P., Parker, D. F. (2010). Omni-directional Rayleigh, Stoneley and Schölte waves with general time dependence. *Proc. R. Soc. A*, 466, 2241-2258.
- [10] Knowles, J. K. (1966). A note on elastic surface waves. *J. Geophys. Res.*, 71, 5480-5481.
- [11] Kaplunov, J. D. and Kossovich, L. Y. (2004). Asymptotic model of Rayleigh waves in the far-field zone in an elastic half-plane. *Dokl. Phys.*, 49, 234-236.
- [12] Kaplunov, J. D., Kossovich, L., and Zakharov, A. (2004). An explicit asymptotic model for the Bleustein-Gulyaev wave. *C. R. Mecanique*, 332, 487-492.

- [13] Kaplunov J., Zakharov A. and Prikazchikov D. A. (2006). Explicit models for elastic and piezoelectric surface waves. *IMA J. Appl. Math.*, 71, 768–782.
- [14] Dai, H. H., Kaplunov J. and Prikazchikov D.A. (2010). A long-wave model for the surface elastic wave in a coated half-space. *Proc. R. Soc. A.*, 466, 3097–3116.
- [15] Kaplunov, J., Nolde, E. and Prikazchikov, D. A. (2010). A revisit to the moving load problem using an asymptotic model for the Rayleigh wave. *Wave Motion*, 7, 1440–451.
- [16] Fryba, L. (1999). *Vibration of solids and structures under moving loads*. London: Thomas Telford.
- [17] Georgiadis, H. G. and Lykotrafitis, G. (2001). A method based on the Radon transform for three-dimensional elastodynamic problems of moving loads. *Journal of elasticity and the physical science of solids*, 65, 87–129.
- [18] Vladimirov, V. S. (1971). *Equations of mathematical physics*. New York: M. Dekker.
- [19] Gelfand, I. M. and Shilov, G. E. (1964). *Generalized functions*. Vol. 2. New York: Academic Press.
- [20] Taylor, M. E. (1996). *Partial differential equations II: Qualitative studies of linear equations*. Springer.
- [21] Hörmander, L. (1987). *The analysis of linear partial differential operators III: Pseudo-differential operators*. Springer.
- [22] Bitsadze, A. V. (1980). *Equations of mathematical physics*. Moscow: Mir Publishers.
- [23] Achenbach, J. D. (1973). *Wave propagation in elastic solids*. Amsterdam: North-Holland.
- [24] Gould, P. L. (1999). *Introduction to linear elasticity*. Berlin: Springer Verlag.
- [25] Graff, K. F. (1991). *Wave motion in elastic solids*. New York: Dover Publications.

- [26] Miller, P. D. (2006). Applied asymptotic analysis. Rhode Island: American Mathematical Society.
- [27] Murray, J. D. (1974). Asymptotic analysis. New York: Siproinger-Verlag.
- [28] Kaplunov J., Prikazchikov D. A., Erbaş, B., Şahin, O. (2013). On a 3D moving load problem for an elastic half space. *Wave Motion*, 50, 1229 –1238.
- [29] Cole, J. H. (1958). Stresses produced in a half plane by moving loads. *J. Appl. Mech.*, 25, 433–436.
- [30] Sidorov, Y. V., Fedoryuk M. V. and Shabunin, M. I. (1985). Lectures on the theory of functions of a complex variable. Moscow: Mir Publishers.
- [31] Shuvalov, A. L. and Every, A. G. (2008). On the long-wave onset of dispersion of the surface-wave velocity in coated solids. *Wave Motion*, 45, 857–863.
- [32] Borovikov, V. A. (1994). Uniform stationary phase method. London: Institution of Electrical Engineers.
- [33] Abramowitz, M. and Stegun, I. A. (2012). Handbook of mathematical functions. New York: Dover Publications.
- [34] Poruchikov, V. B. (1992). Methods of the classical theory of elastodynamics. Berlin: Springer-Verlag.
- [35] Kaouri, K., Allwright, D. J., Chapman, C. J., Ockendon, J. R. (2008). Singularities of wavefields and sonic boom. *Wave Motion*, 45, 217–237.

CURRICULUM VITAE

Name-Surname : Onur ŞAHİN
Foreign Language : English
Date and Place of Birth : 15 October 1984, Varto/Muş
E-mail : onur.sahin@anadolu.edu.tr

Education

- 2004–2008, Dumlupınar University, Faculty of Science, Department of Mathematics, BSc.
- 2008–2010, Dumlupınar University, Graduate School of Sciences, Applied Mathematics, MSc.
- 2011– , Anadolu University, Graduate School of Sciences, Applied Mathematics, PhD.

Work Experience:

- 2010–2011, Giresun University, Faculty of Science, Department of Mathematics.
- 2011– , Anadolu University, Faculty of Science, Department of Mathematics.

Publications:

- Kaplunov, J., Prikazchikov, D. A., Erbaş, B., Şahin, O. (2013). On a 3D moving load problem in an elastic half space. Wave Motion, 50: 1229–1238.
- Erbaş, B., Prikazchikov, D. A., Kaplunov, J., Şahin, O. (2014). The near-resonant regimes of a moving load in a three-dimensional problem for a coated elastic half-space. Math. Mech. Solids. doi:10.1177/1081286514555451.

Conference Presentations:

- 2013, An approximate solution of the 3D moving load problem for an elastic half space based on the explicit model for the Rayleigh wave, Day on Diffraction, St. Petersburg Rusya.
- 2013, An asymptotic model for a 3D moving load problem for uncoated and coated elastic half-spaces, VI th International Workshop on Differential Equations and Applications, İzmir Turkey.
- 2015, An investigation of the asymptotic solution of the 3D moving load problem for a coated half space, Euromech Colloquium 574 Recent Trends in Modeling of Moving Loads on Elastic Structures, Eskişehir Turkey.

Research Grants:

- 2013–2015, Anadolu University, Research Projects no: 1306F268. Elastic surface waves for coated structures–Resonance case for moving load problems.
- 2013, Anadolu University, Research Projects no: 1306F208. Moving load problems in dynamical elasticity.

Association Membership:

- 2015–2016, European Mechanics Society.